

摩擦抵抗低減効果を持つ
機能性船底塗料の数値解析

Numerical simulation for functional
painting of ship hull with friction drag
reduction effect

応用流体力学グループ

高木 洋平

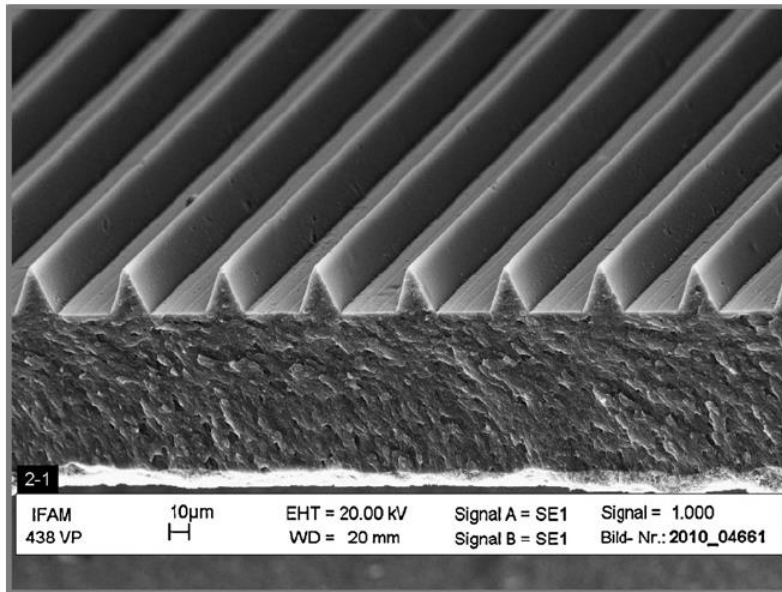
Research group of applied hydrodynamics

Y. Takagi

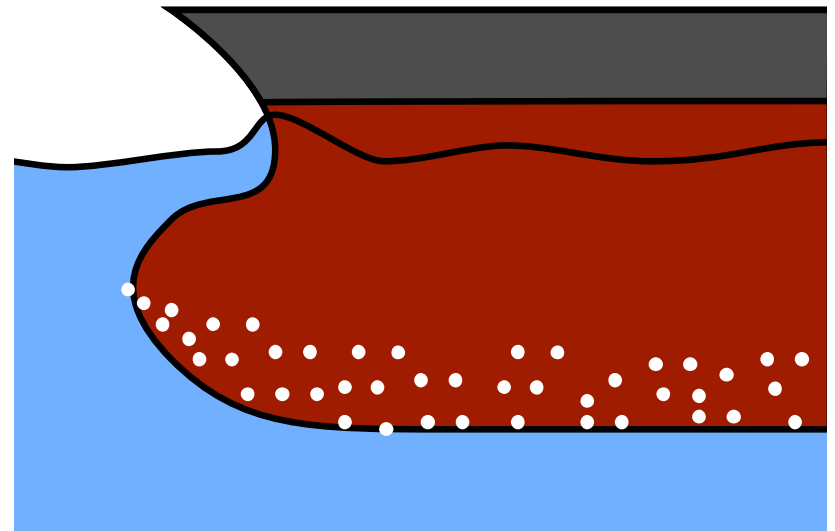
Turbulent drag reduction

- Applications in wall turbulence

Riblet



Micro bubble

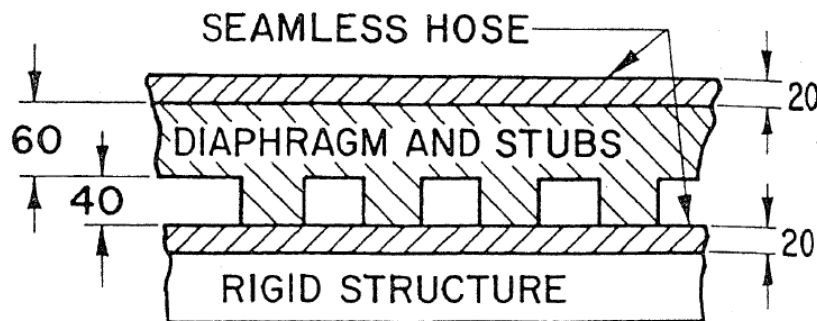


Stenzel *et al.*, Prog. Org. Coat. (2011)

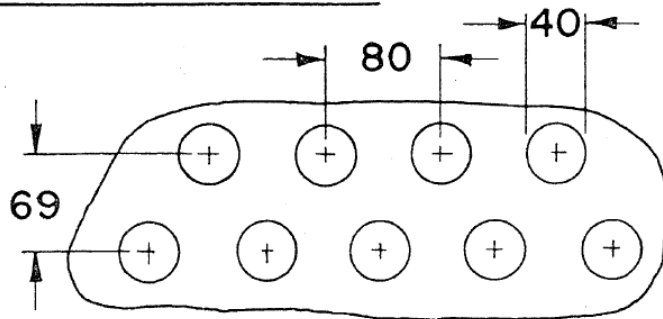
Turbulent drag reduction

Compliant surface

CROSS SECTION



CUT THROUGH STUBS



M. O. Kramer, J. American Soc.
Naval Eng. (1960)

Requirement for ship hull:

- Easy-to-use
- Durability
- Low cost

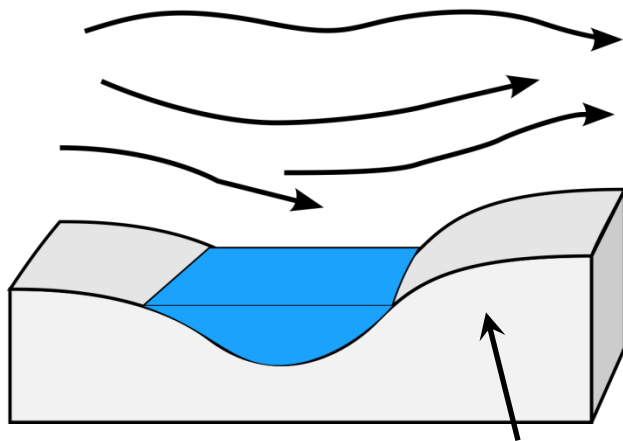
Painting is usually used for anti-fouling.



Functional painting with drag reduction effect

Commercial painting

- LF-Sea (Nippon Paint)
 - Hydrogel formation
 - DR $\sim 10\%$
 - Biomimetic
 - Water trapping effect

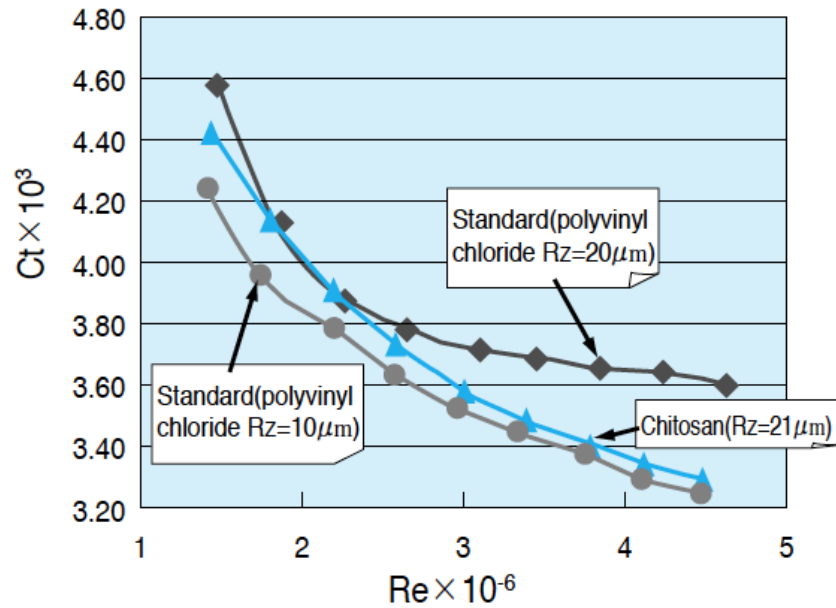


Water trapped layer



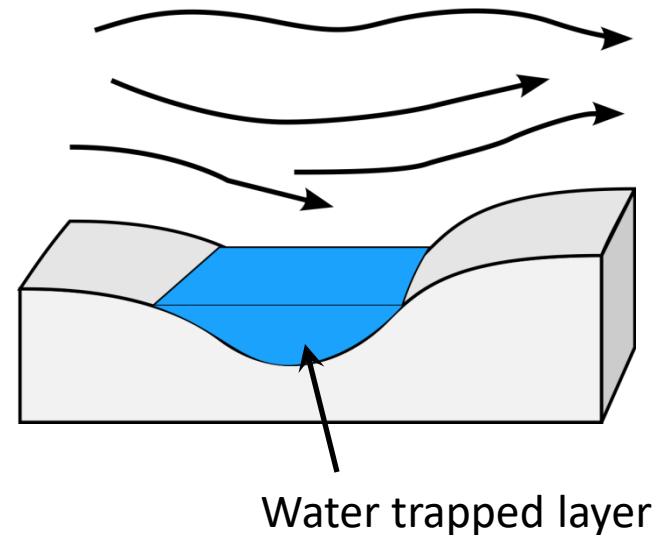
Drag reduction effect with hydrogel

Result of towing tank test



山盛, TECHNO-COSMOS, 2005

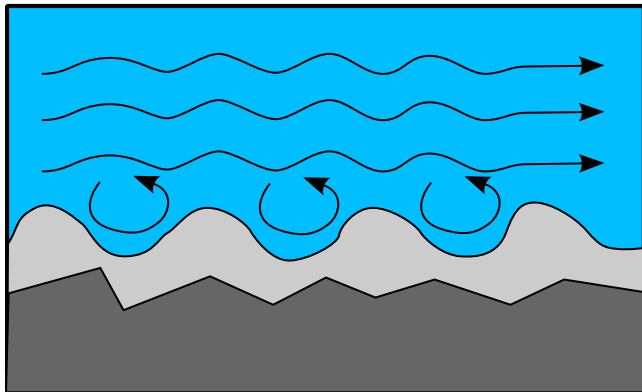
Proposed drag reduction mechanism



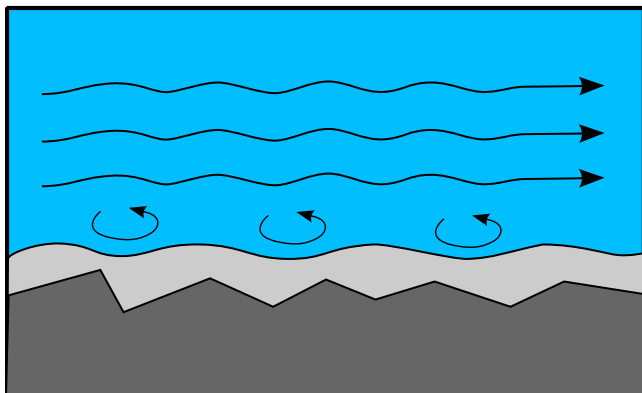
山盛&島田, TECHNO-COSMOS, 2009

Painting condition in sea water

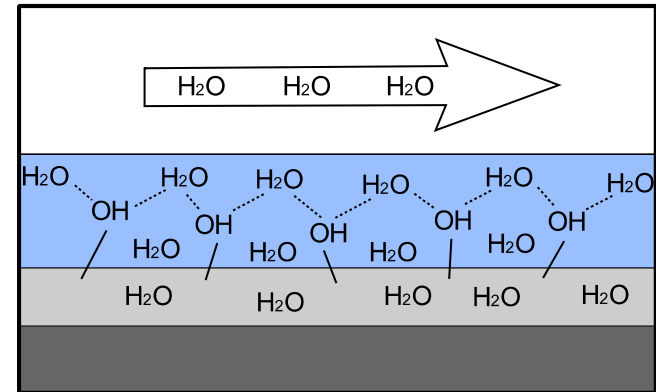
Self-polishing type



after shipping

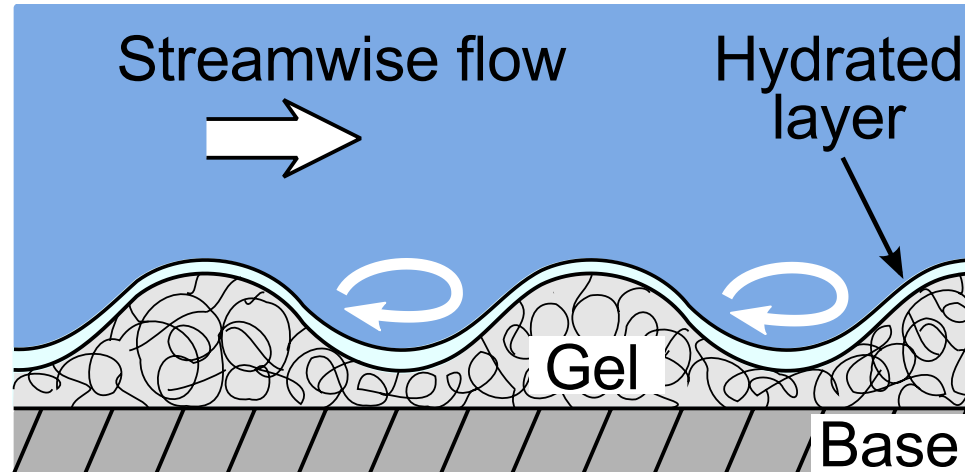


Hydration type



- Green
- Stress relaxation

Structures around hydrogel painting

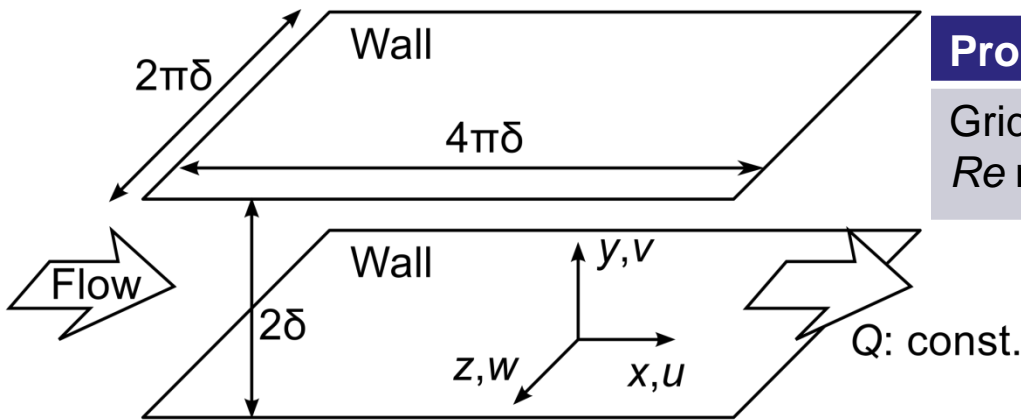


Proposed mechanism for drag reduction

1. Slip velocity due to water trapping
2. Stress relaxation due to compliant gel polymer
3. Surface deformation and roughness
4. Water penetration into hydrated and gel layers (porous-like structure)

1. Slip velocity due to water trapping:
numerical modeling in plane channel flow

Direct Numerical Simulation (DNS) of turbulent channel flow



| Property | Symbol | Value |
|-------------|-----------------------------|-----------------------------|
| Grid number | $N_x \times N_y \times N_z$ | $128 \times 151 \times 128$ |
| Re number | $Re_C (Re_\tau)$ | 4200 (180) |

Governing equations

Navier-Stokes equation:

$$\frac{\partial u_i}{\partial t} + \frac{\partial (u_i u_j)}{\partial x_j} = -\frac{1}{\rho} \frac{\partial p}{\partial x_i} + \frac{1}{Re} \frac{\partial^2 u_i}{\partial x_j^2}$$

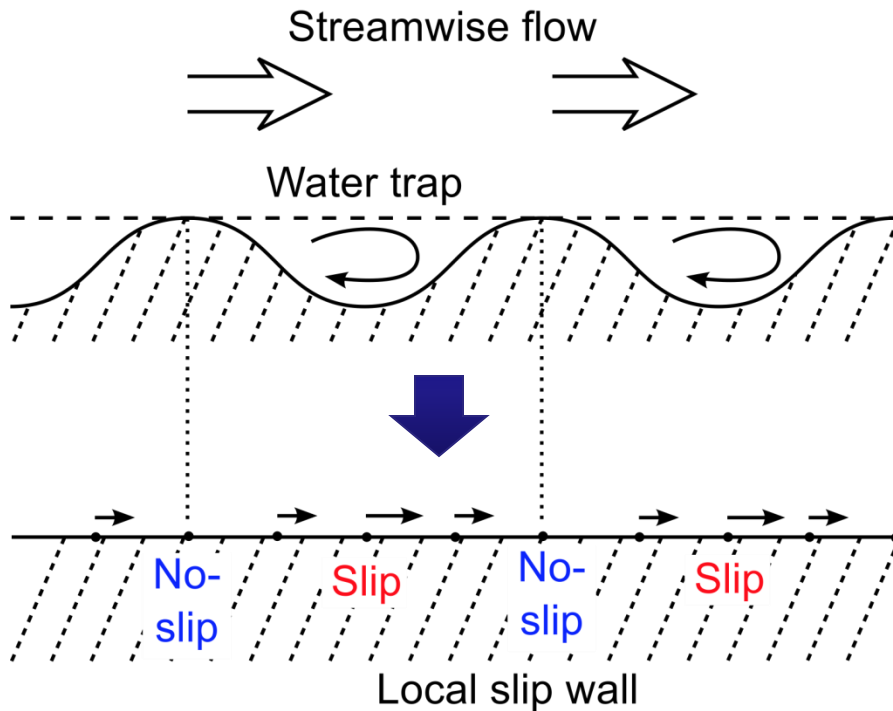
Continuity equation:

$$\frac{\partial u_i}{\partial x_i} = 0$$

Numerical scheme

- 2nd-order Finite Difference Method
- Crank Nicholson for viscous term
- 3rd-order Runge-Kutta
- Poisson eq. in Fourier space was solved by TDMA.

Slip velocity condition



Local slip velocity

$$u_s = l_x \frac{\partial u}{\partial y}, w_s = l_z \frac{\partial w}{\partial y}$$

where

$$l_x, l_z = f_x f_z l_0$$

$$f_x = \frac{1}{2} \left\{ 1 + \cos \left(\frac{2\pi}{\lambda_x} x \right) \right\},$$

$$f_z = \frac{1}{2} \left\{ 1 + \cos \left(\frac{2\pi}{\lambda_z} z \right) \right\}$$

| Property | Value |
|-----------------------------------|--------------------------|
| Reference slip length (l_0^+) | 0.36 |
| Slip wave length: | |
| x-direction (l_x^+) | 275, 368, 550, 735, 1100 |
| z-direction (l_z^+) | 50, 100, 183, 367 |

Validation of simulation code

Drag reduction ratio (DR) under uniform slip velocity condition

| Case | Slip length | DR (Min & Kim[1]) | DR (Present) |
|-----------------|---------------------------|----------------------|-----------------|
| Streamwise slip | $l_x^+ = 0.36, l_z^+ = 0$ | 5% | 5.5% |
| Spanwise slip | $l_x^+ = 0, l_z^+ = 0.36$ | -3% | -3.6% |
| Isotropic slip | $l_x^+ = l_z^+ = 0.36$ | -1% | -0.6% |

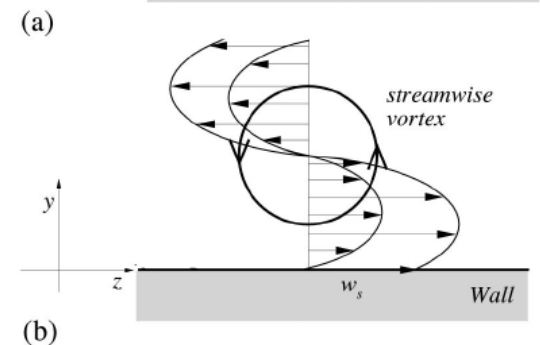
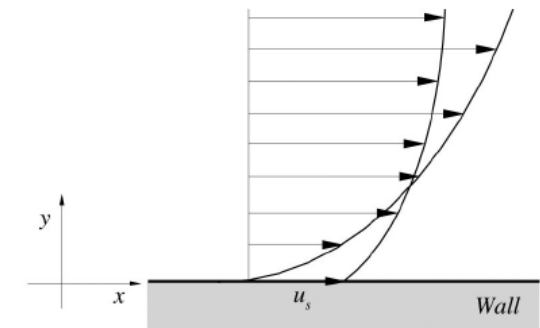
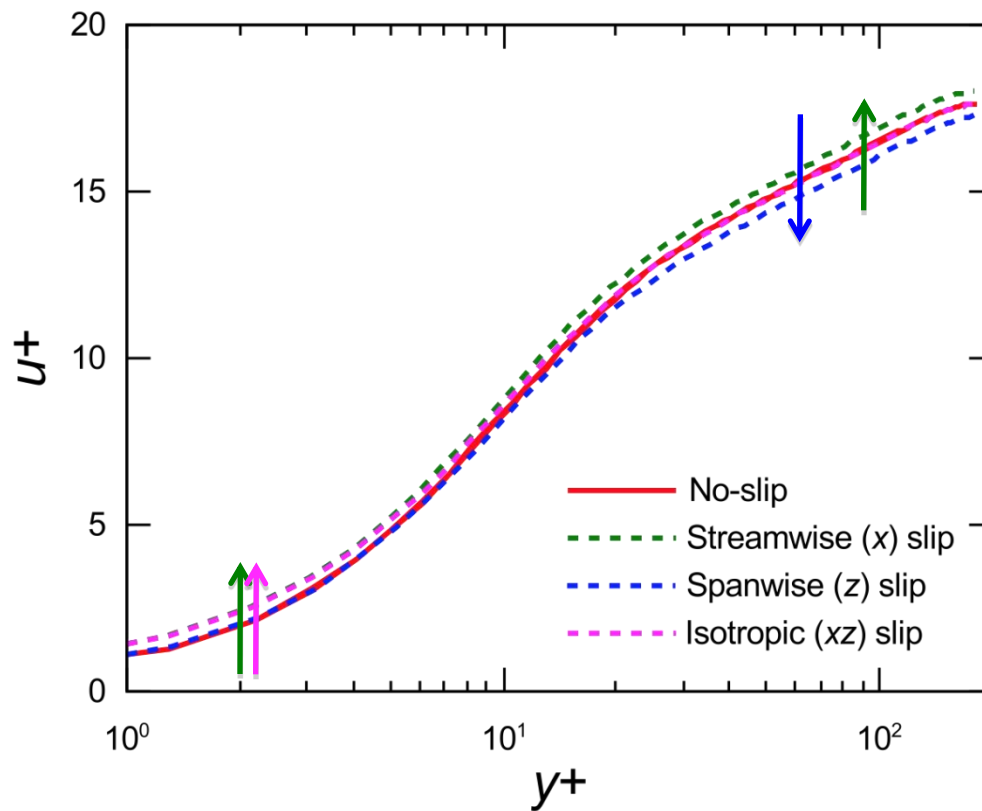
[1] T. Min and J. Kim, Phys. Fluids, 16(7), L55 (2004).

Drag reduction ratio

$$DR[\%] = \frac{\left(-\frac{dp}{dx} \Big|_{\text{no-slip}} \right) - \left(-\frac{dp}{dx} \Big|_{\text{slip}} \right)}{\left(-\frac{dp}{dx} \Big|_{\text{no-slip}} \right)} \times 100$$

Validation of simulation code

Mean velocity profiles under uniform slip velocity condition

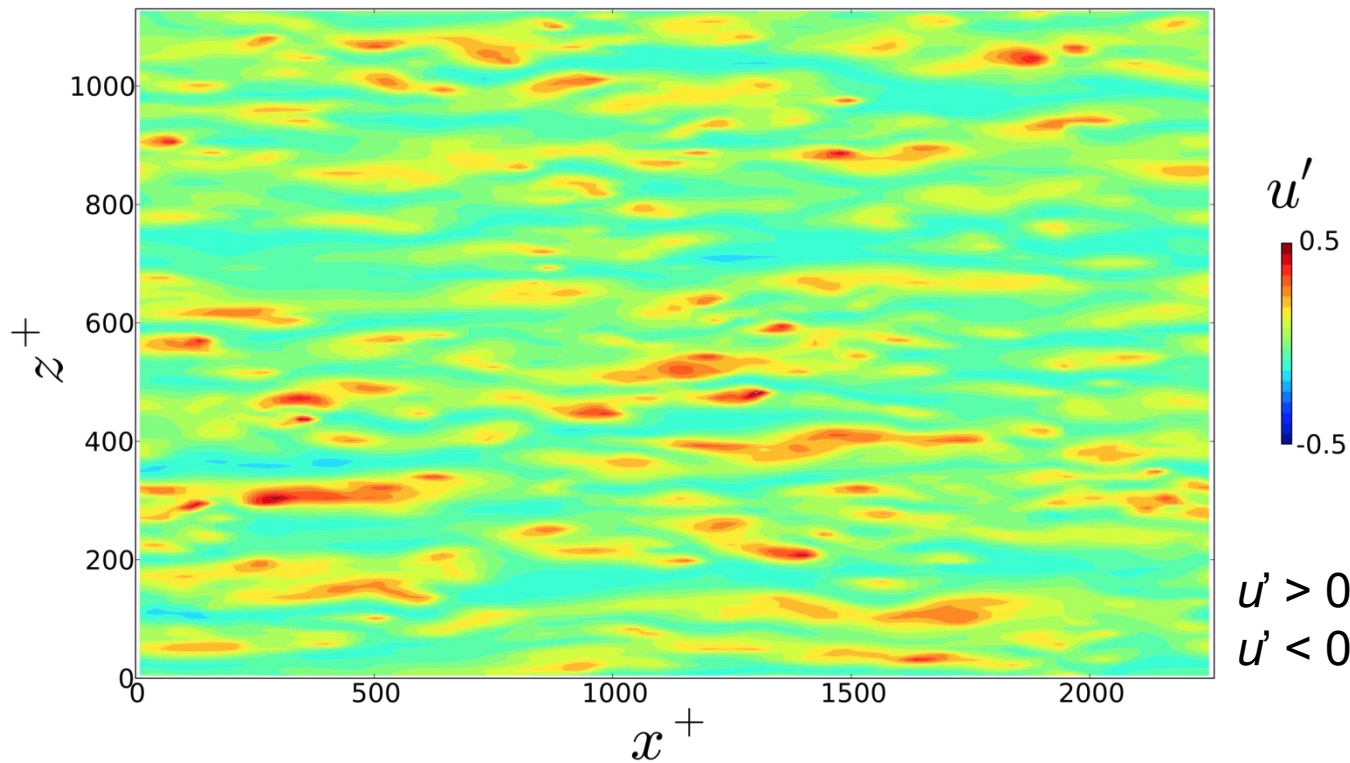
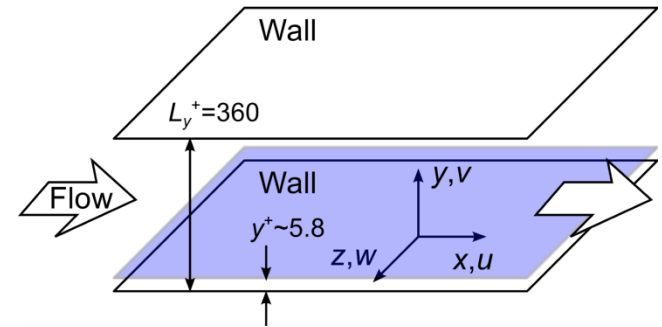


Drag decrease/increase mechanism (Min&Kim, 2004)

Streak structure

Streamwise velocity fluctuation at $y^+ \sim 5.8$

$$u'(y, t) = u(x, y, z, t) - \langle u(x, y, z, t) \rangle_{xz}$$

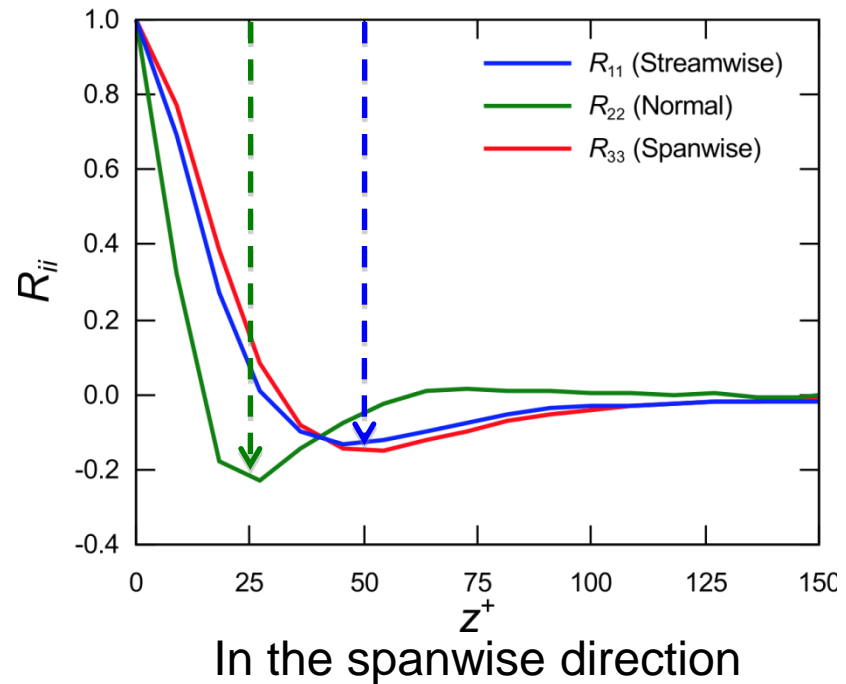
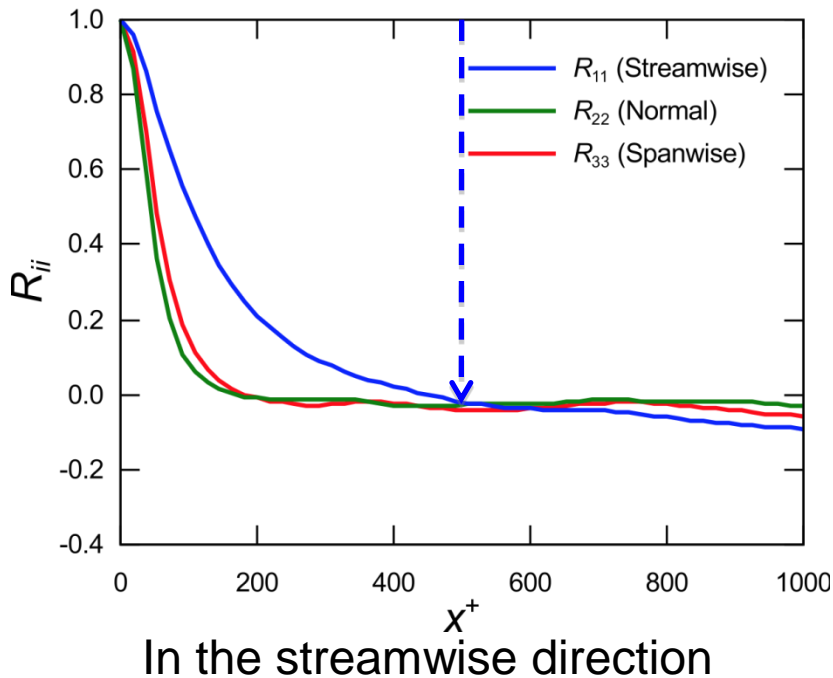


$u' > 0$: high speed streak
 $u' < 0$: low speed streak

Scale of streak structures

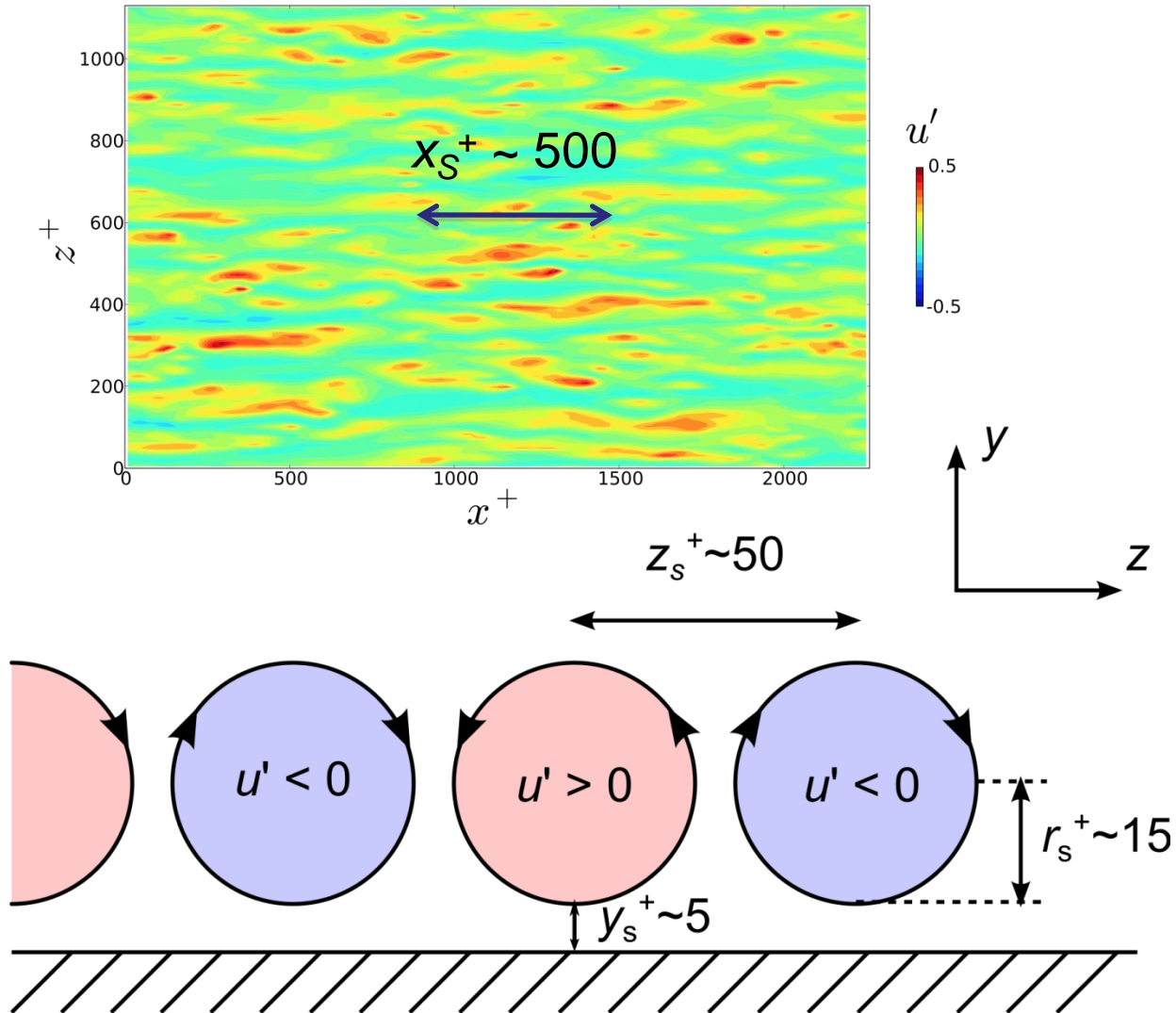
Two-point correlations at $y^+ \sim 5.8$

$$R_{ii}(r_1) = \frac{\langle u'_i(x, y, z)u'_i(x + r_1, y, z) \rangle}{\langle u_i'^2(x, y, z) \rangle}, R_{ii}(r_3) = \frac{\langle u'_i(x, y, z)u'_i(x, y, z + r_3) \rangle}{\langle u_i'^2(x, y, z) \rangle}$$

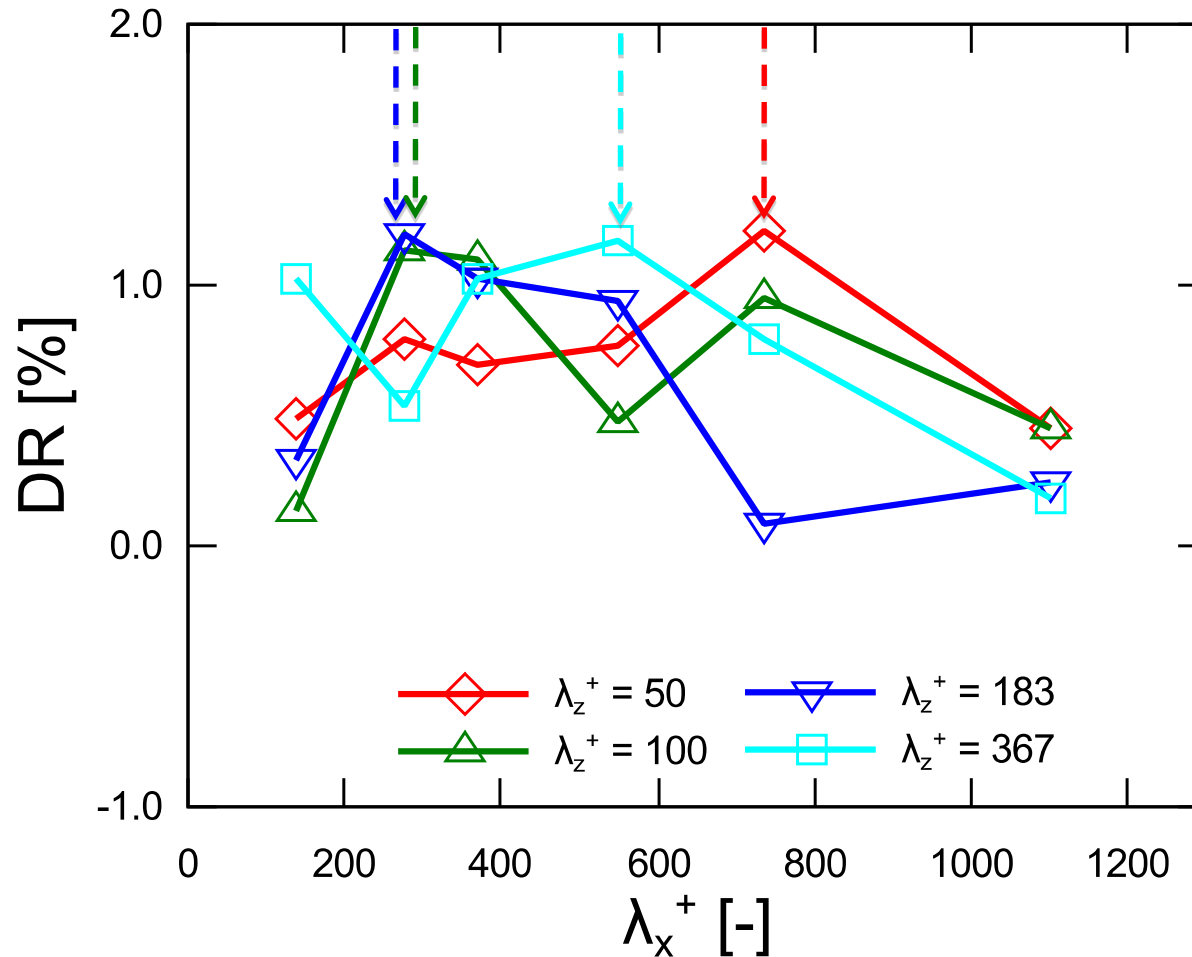


Negative correlation is related with the scale of high/low streaks.

Scale of streak structures



Dependency of local slip velocity



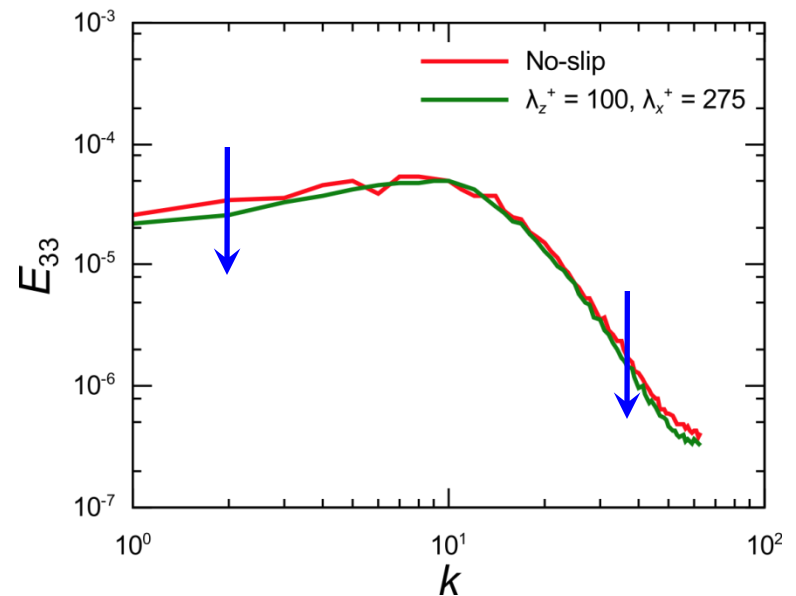
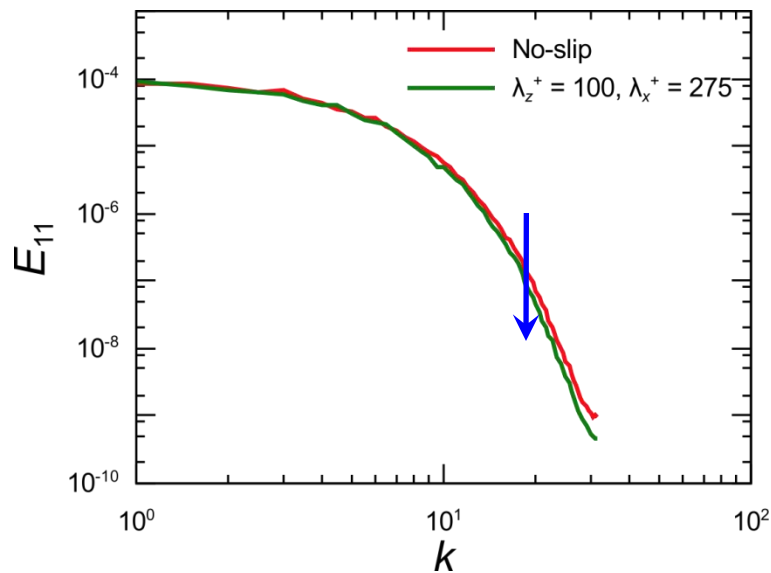
Optimum local slip condition was not specified uniquely.

Suppression of energy dissipation

One-dimensional energy spectra at $y^+ \sim 5.8$

$$E_{11}(k) = \int_{-\infty}^{+\infty} u'_i(x, y, z) u'_i(x+r, y, z) e^{-ikr} dr$$

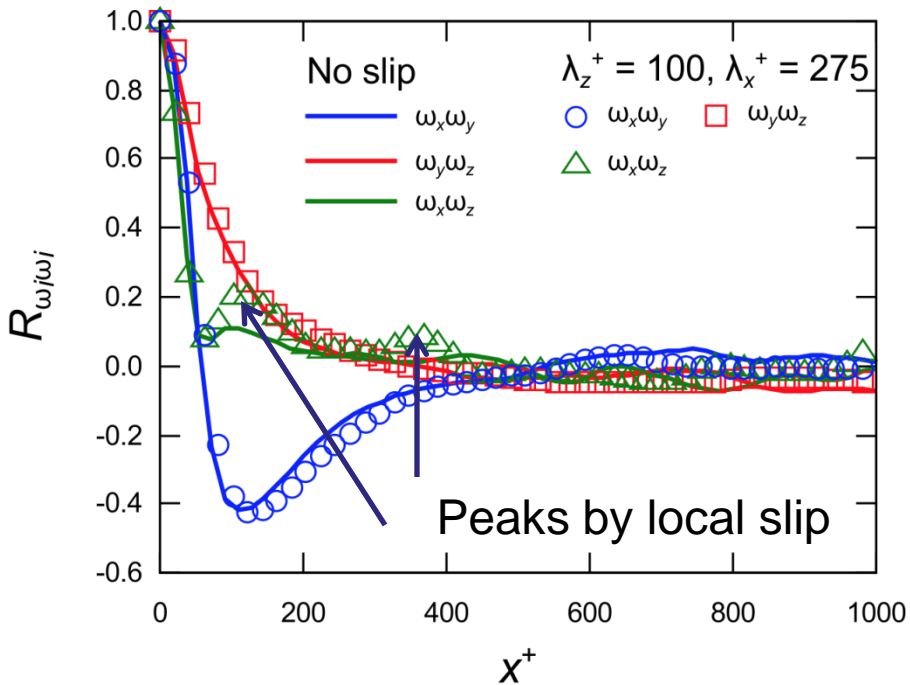
$$E_{33}(k) = \int_{-\infty}^{+\infty} u'_i(x, y, z) u'_i(x, y, z+r) e^{-ikr} dr$$



The spanwise intensity of streak structure decreased by local slip.

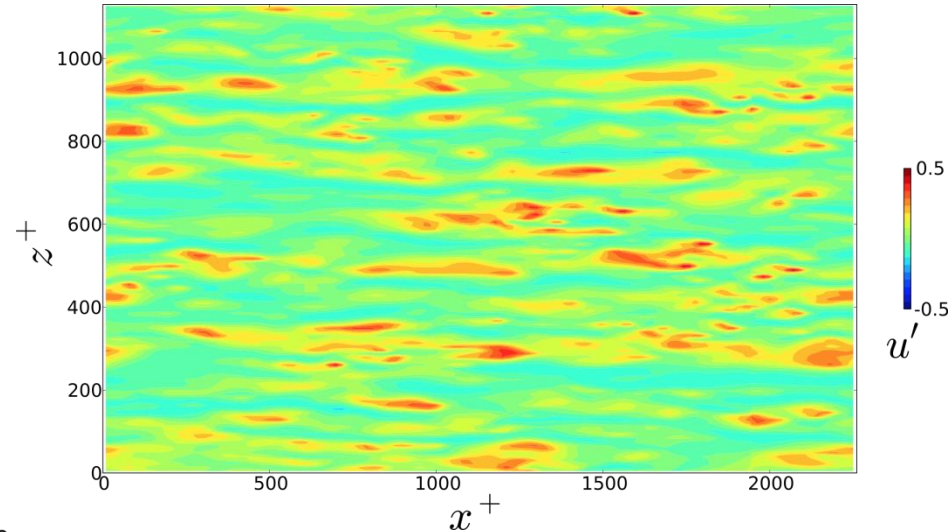
Vortex interaction

Two-point correlation of vorticity



Vortex interaction was seen in the horizontal plane.

Velocity fluctuation (streak structure)



No significant change

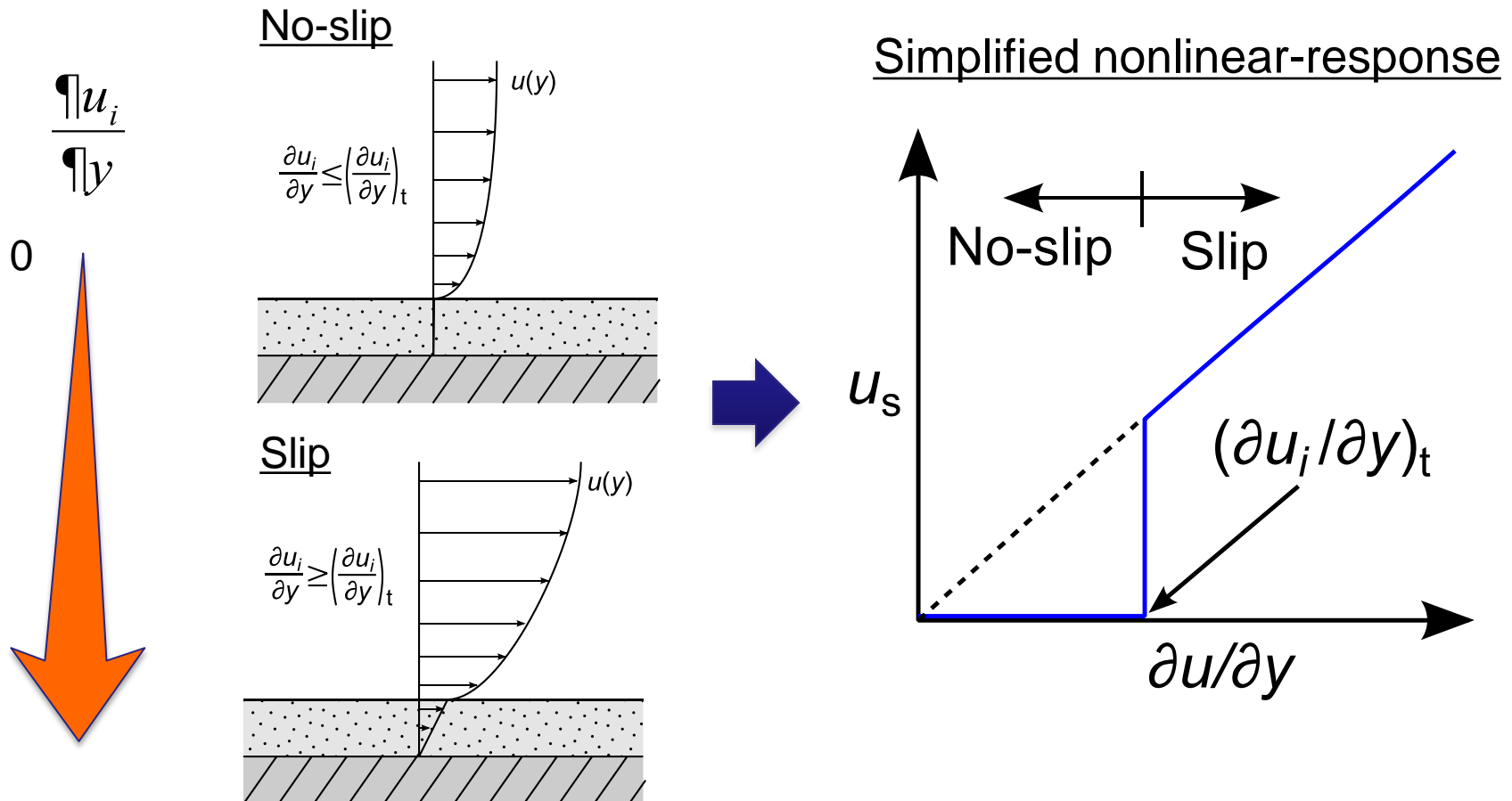
Summary of topic 1

- A turbulent channel flow simulation with **local slip velocity** was carried out.
- The slip wavelength compared with the **size of streak structure** was **effective** for drag reduction.
- The **spanwise energy dissipation** related with the streak scale was selectively **suppressed**.
- The **vortex interaction** was seen in the streamwise and spanwise directions. However, it did not lead to drag increase.

2. Stress relaxation due to compliant gel polymer: Nonlinear response of hydrogel to shear stress

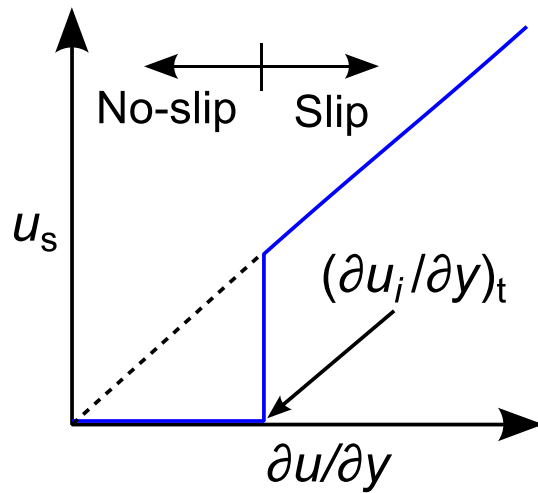
Response to high wall shear stress

- Gel: nonlinear stress response

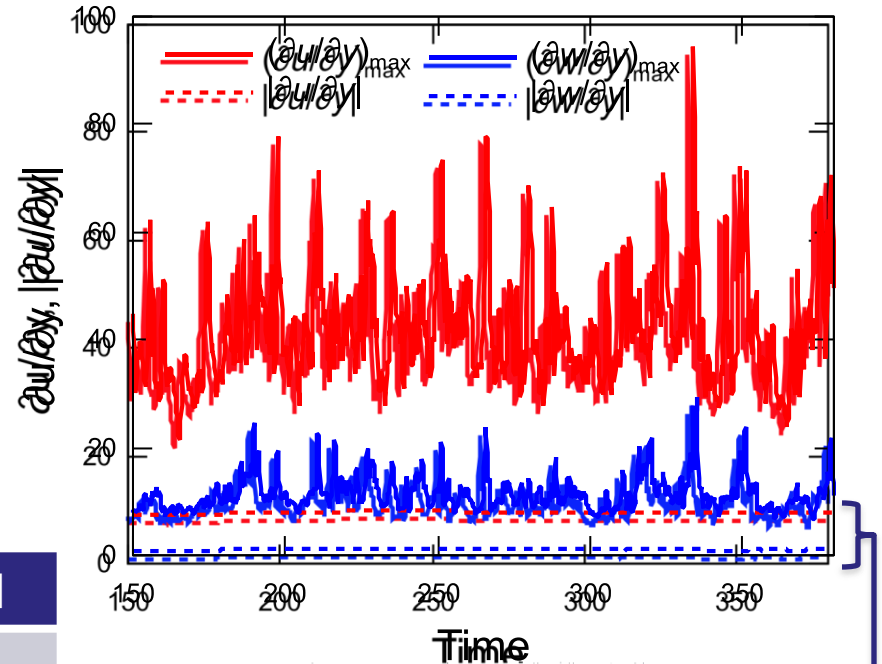


Threshold of slip condition

Nonlinear stress response



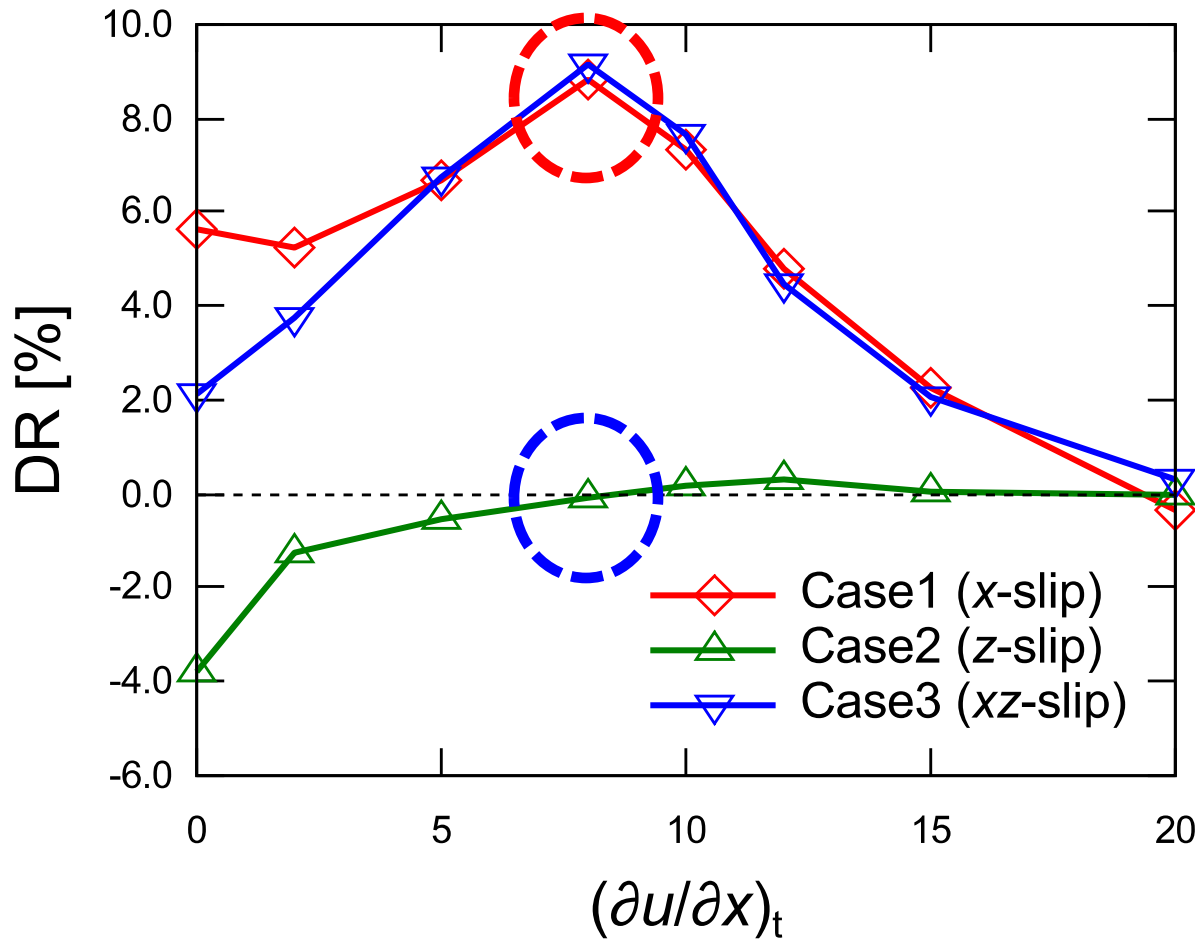
Calculated range of velocity gradient on wall (no-slip case)



| Label | Type | Threshold |
|--------|---------------------|-----------|
| Case 1 | only x-slip | 0 ~ 20 |
| Case 2 | only z-slip | |
| Case 3 | isotropic (xz-slip) | |

$$\left\langle \frac{\eta u}{\eta y} \right\rangle \sim 8, \quad \left\langle \frac{\eta w}{\eta y} \right\rangle \sim 1$$

Dependency of drag reduction



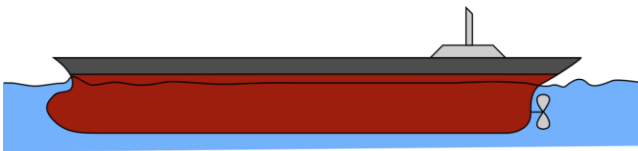
$$DR[\%] = \frac{\left(-\frac{dp}{dx} \Big|_{\text{no-slip}} \right) - \left(-\frac{dp}{dx} \Big|_{\text{slip}} \right)}{\left(-\frac{dp}{dx} \Big|_{\text{no-slip}} \right)} \times 100$$

Total slip effect was given by the summation of each contribution.

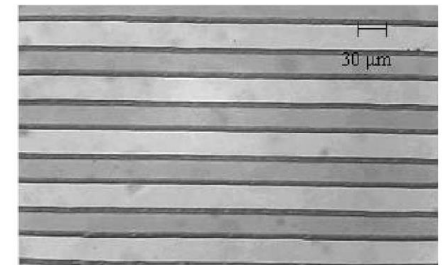
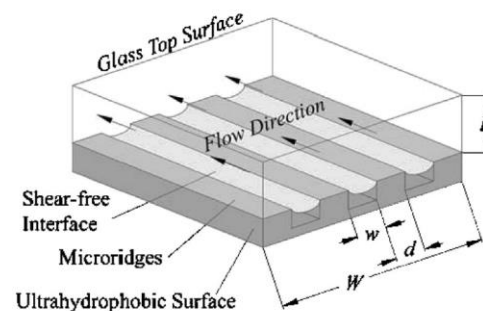
Summary of topic 2

- A three-dimensional simulation considering shear stress response in hydrogel was carried out.
- Although the stress response was isotropic, significant drag reduction effect was achieved.
- Isotropic hydrogel painting might be useful for wall turbulence with the change of streamwise direction.

In oblique flow



Super hydrophobic flow

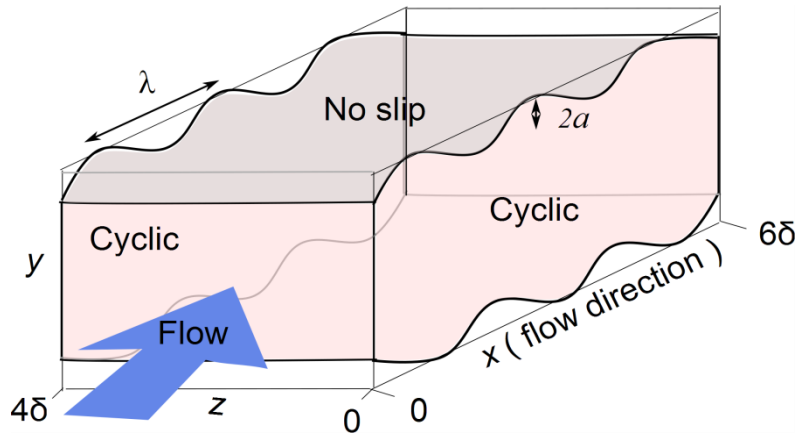


3. Surface deformation and roughness: wavy channel flow simulation

Numerical condition

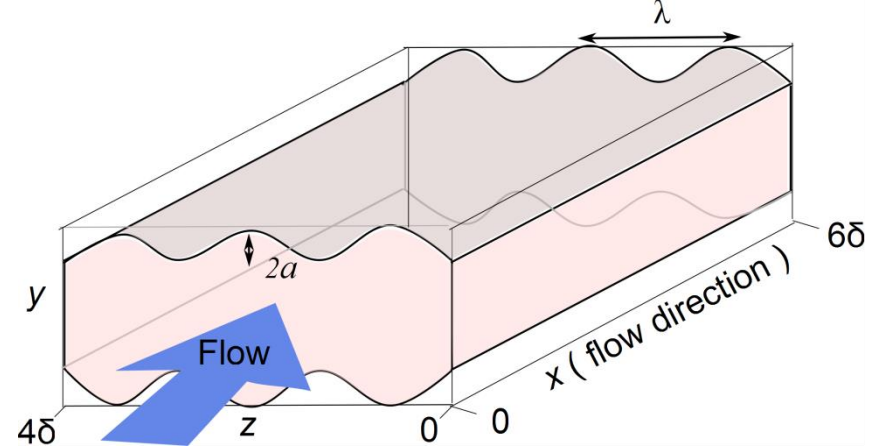
Streamwise wavy channel

Case 1



Spanwise wavy channel

Case 2 : $\lambda = 1.33$ m, Case 3 : $\lambda = 0.1$ m



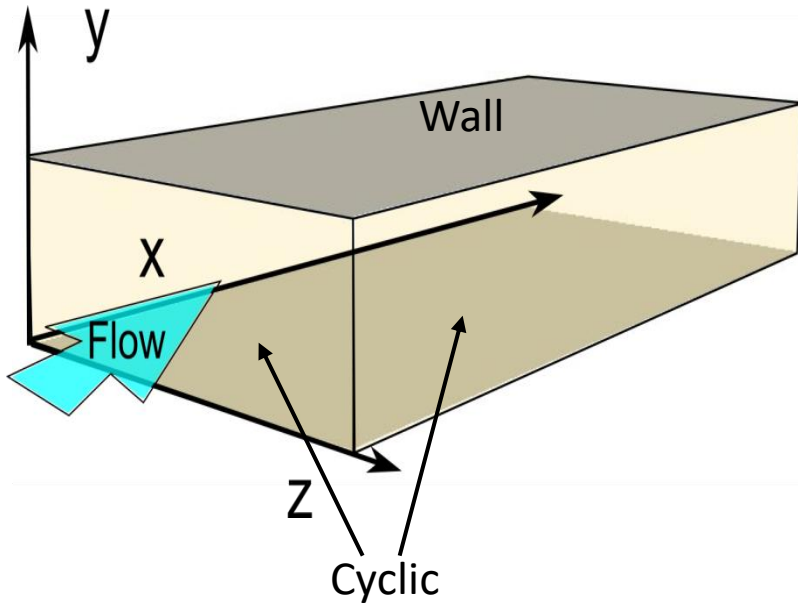
Wave shape of the wall : $y = a \left\{ 1 + \cos \left(\frac{2\pi}{\lambda} x \right) \right\}$ δ : channel-half width

| | Case1 | Case2 | Case3 |
|------------------------------|-------------|-------------|-------------|
| Wave type | streamwise | spanwise | |
| Wave length(λ) [m] | 2.0 | 1.33 | 0.1 |
| Amplitude(a) [m] | 0.1δ | 0.1δ | 0.1δ |
| Grid Number(x, y, z) | 148,95,128 | 128,95,148 | 129,97,241 |

Code validation

DNS of a turbulent channel flow by using **OpenFOAM**[®]

No turbulence model



| Label | Grid number | Method |
|----------------------------------|---------------------|------------------|
| Kim et al. (1987) ^[1] | 192 × 129 × 1 60 | Fourier-spectral |
| Coarse | 64 × 64 × 64 | |
| Middle | 96 × 96 × 96 | FVM with OF |
| Fine | 128 × 128 × 1 28 | |

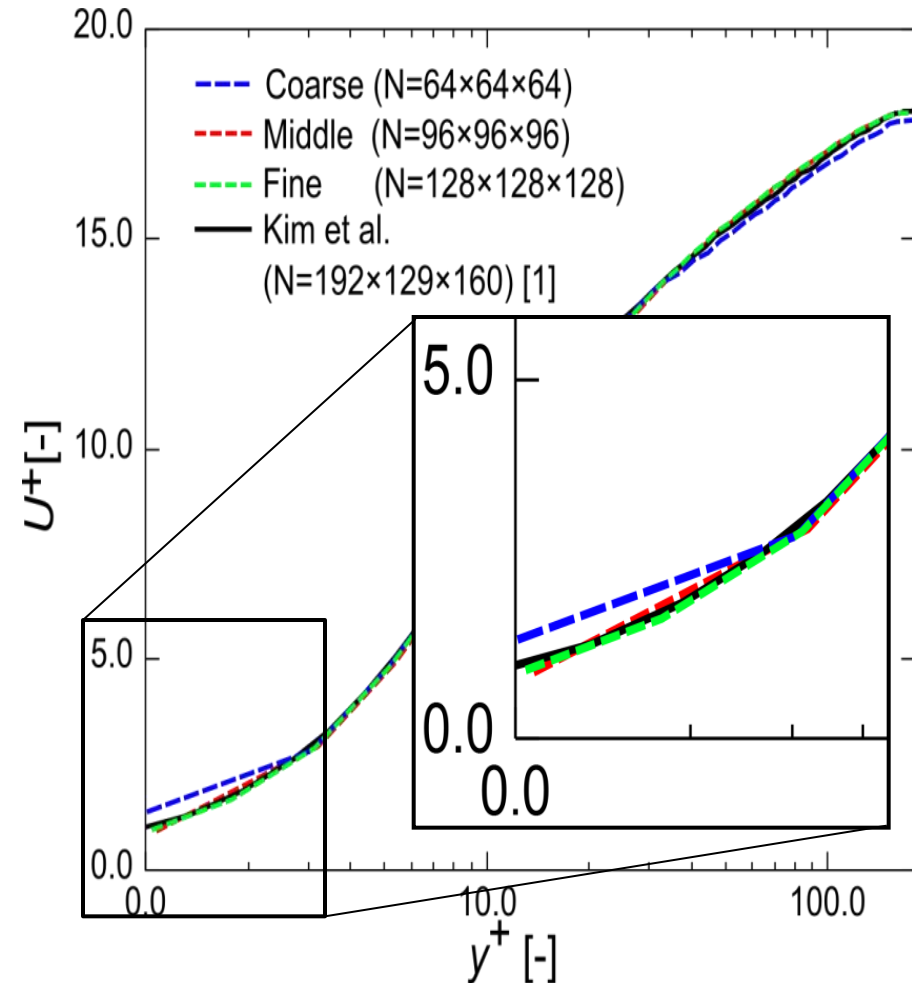
[1] J. Kim et al., *J. Fluid Mech.*, **177**, pp. 133-186 (1987).

$$Re = \frac{2u_m \delta}{\nu} = 5600$$

u_m : mean velocity
 δ : channel-half width
 ν : kinematic viscosity

Code validation

Mean velocity profiles



| | Coarse | Middle | Fine |
|----------------|--------|--------|------|
| Averaged y^+ | 0.60 | 0.51 | 0.49 |

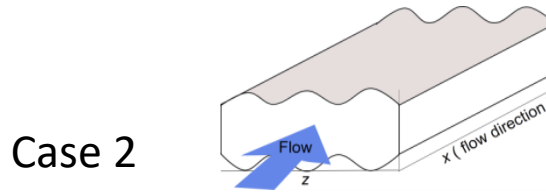
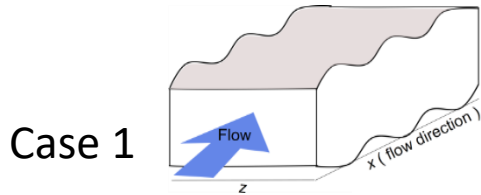
Middle and **Fine** resolution showed good agreements.

OpenFOAM is available for DNS on a turbulent channel flow.

Drag reduction ratio (DR)

$$DR = \frac{\left(-\frac{dP}{dx} \Big|_{flat} \right) - \left(-\frac{dP}{dx} \Big|_{wavy} \right)}{\left(-\frac{dP}{dx} \Big|_{flat} \right)}$$

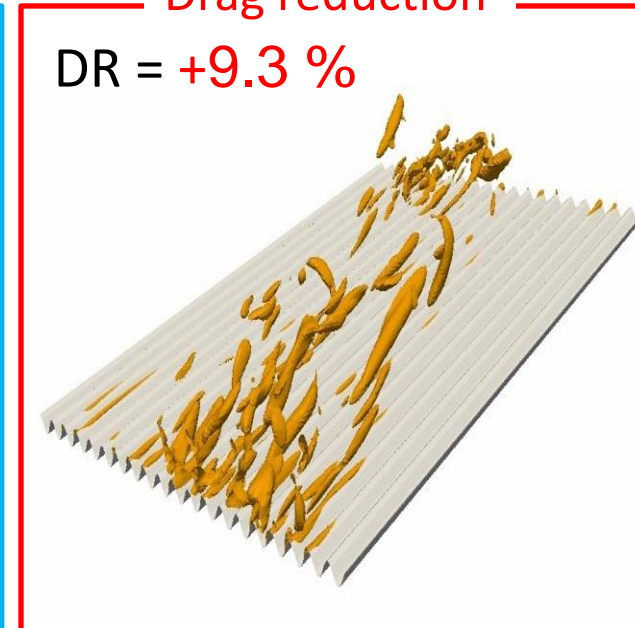
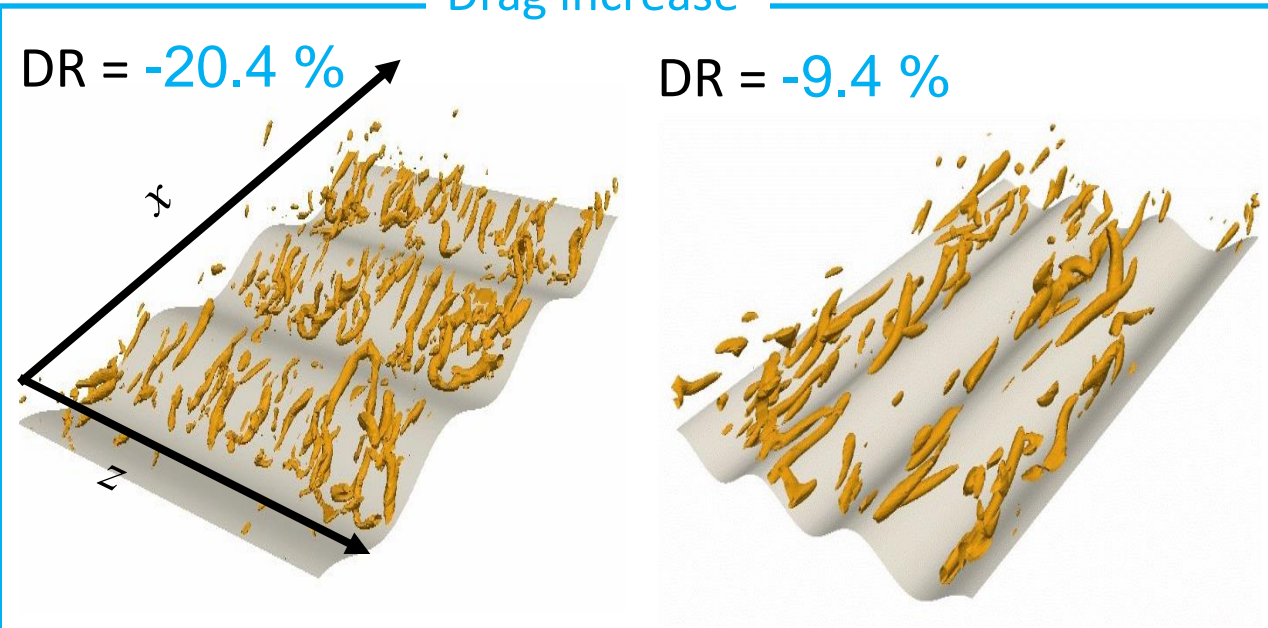
$-\frac{dP}{dx} \Big|_{flat}$: mean pressure gradient in a flat channel
 $-\frac{dP}{dx} \Big|_{wavy}$: mean pressure gradient in a wavy channel



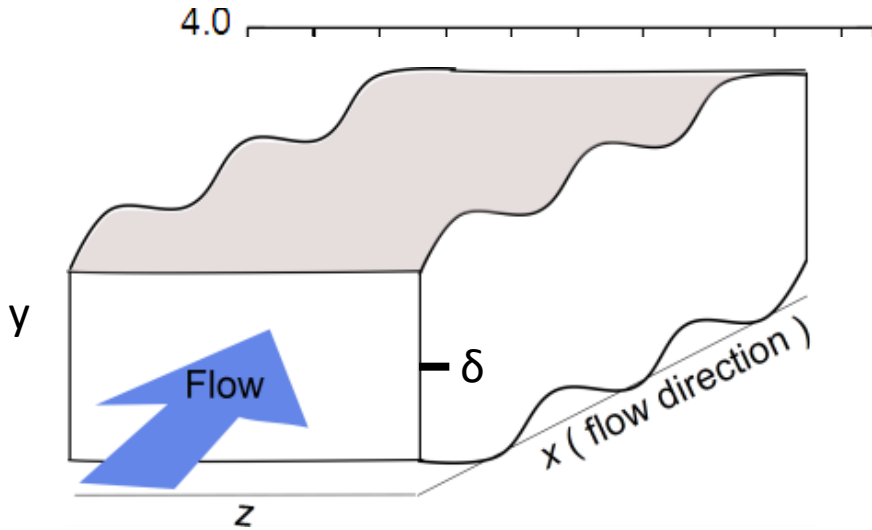
Case 3

Drag increase

Drag reduction

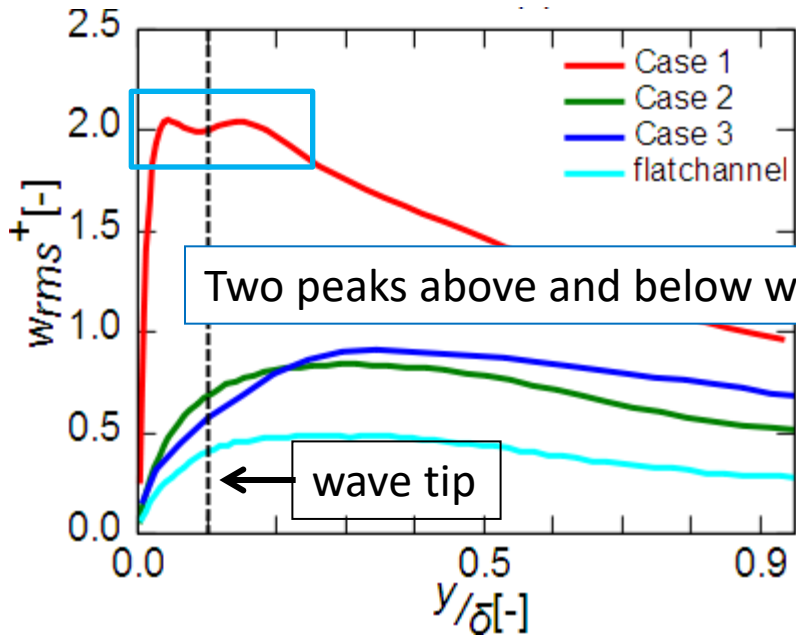


Discussion — Case1 : streamwise wavy channel



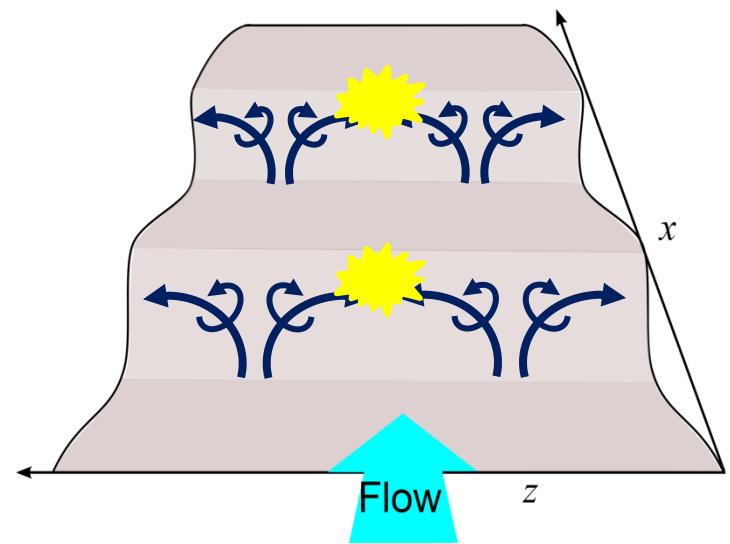
The peak of RMS value profile
➔ **Most random** flow region

δ : channel-half width



Two peaks above and below wave tip

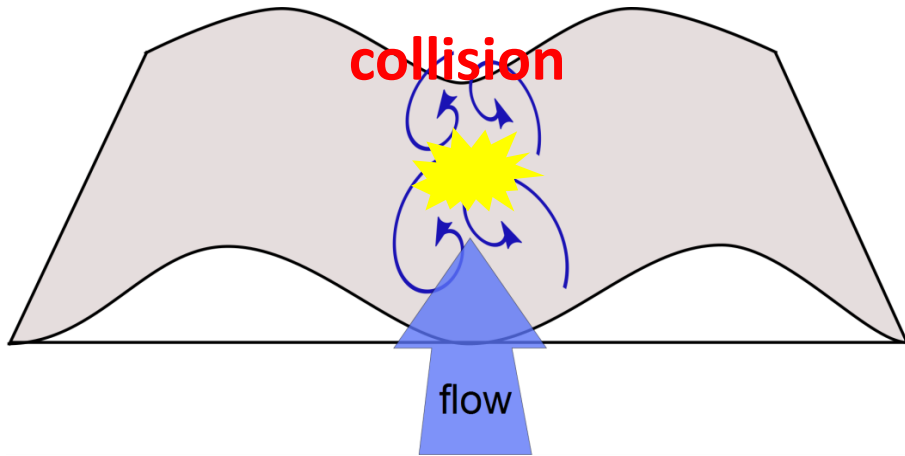
wave tip



Case2 and Case 3 : spanwise wavy channel

Case 2

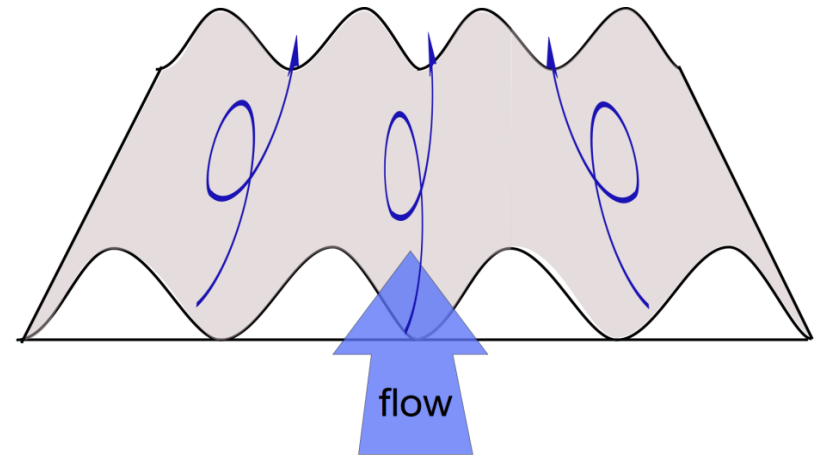
Some vortices in one wave



Advance the dissipation

Case 3

Unit vortex in one wave




Drag reduction

Median diameter of eddies

| | Case1 | Case 2 | Case 3 | Flat channel |
|--------------------------|-------|--------|--------|--------------|
| Median diameter [m] | 0.184 | 0.272 | 0.09 | 0.240 |
| Spanwise wave spacing[m] | — | 1.333 | 0.1 | — |
| DR [%] | -20.4 | -9.4 | +9.3 | 0 |

Summary of topic 3

- **Drag reduction effect** was shown when collision of vortices was suppressed by wall shape.
- **Dissipation** was advanced by collision of **several vortices in one wave** .

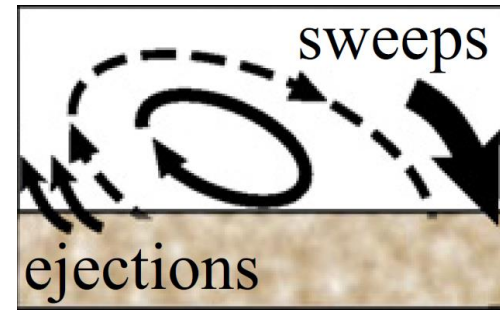
| | Case1 | Case2 | Case 3 |
|--|------------|----------|--------|
| Wave type | Streamwise | Spanwise | |
| Wave length(λ) | 2.0 | 1.33 | 0.1 |
| Median diameter | 0.184 | 0.272 | 0.09 |
| DR [%]  | -20.4 | -9.4 | 9.3 |

Soft matter, Hydrogel, has advantage for drag reduction on ships bottom surface

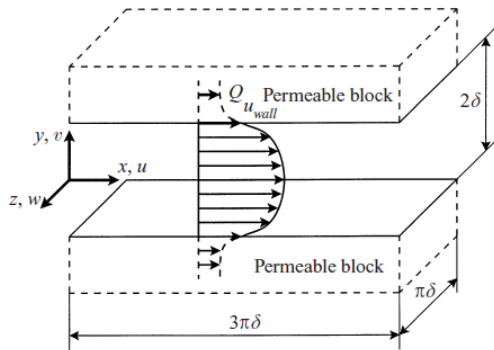
4. Water penetration into hydrated and gel layers (porous-like structure):
channel flow with porous wall

Approaches for fluid flow through porous structure

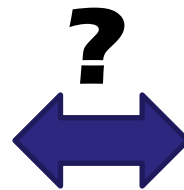
- Experimental research
 - Observation of sweep/ejection near wall¹⁾



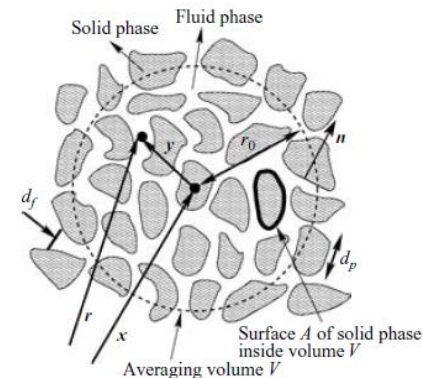
- Numerical research approach²⁾



Increase of turbulent drag



- Continuum approach³⁾

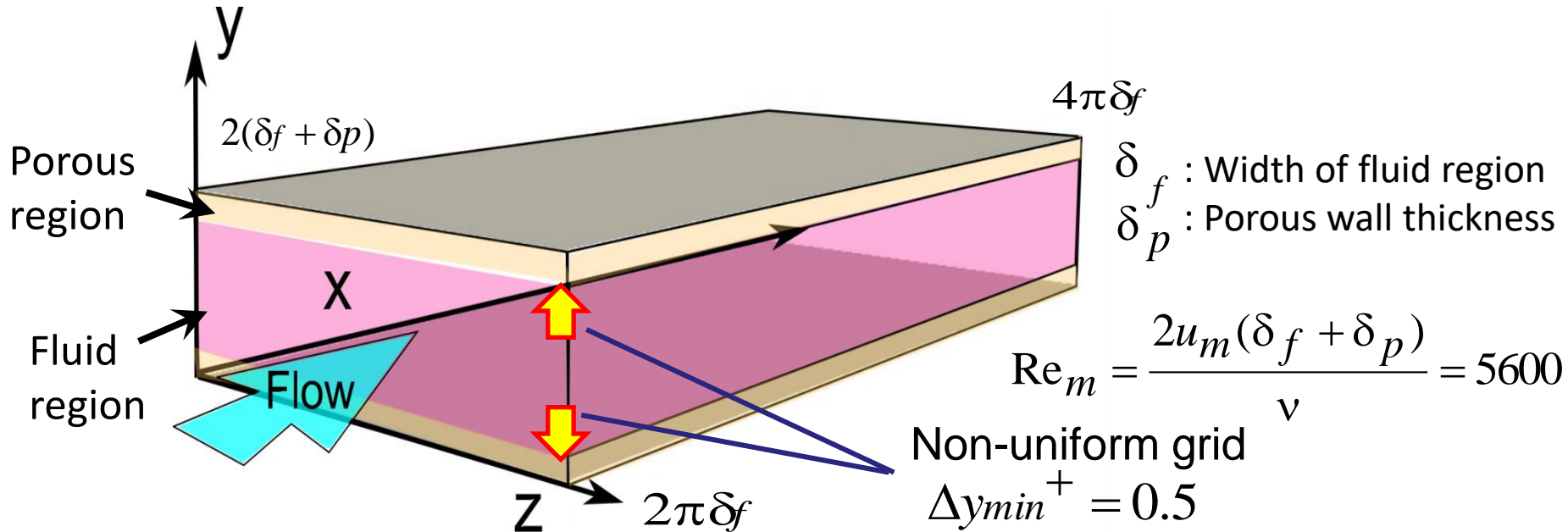


Decrease of skin friction due to **slip velocity**

1) K. Suga et al., *Int. J. Heat Fluid Flow*, 32, 586-595 (2011)
 2) S. Hahn et al., *J. Fluids Mech.* vol. 450, pp. 259- 285(2002)
 3) W. P. Breugem et al., *J. Fluids Mech.* vol. 562, pp. 35-72 (2006)

Numerical conditions

| Case | 5%D | 10%D | 20%D | Flat |
|--|--------------------|--------------------|--------------------|----------------|
| Porous media thickness δ_p | $0.05 \delta_f$ | $0.10 \delta_f$ | $0.20 \delta_f$ | — |
| Total channel width | $2.1 \delta_f$ | $2.2 \delta_f$ | $2.4 \delta_f$ | $2.0 \delta_f$ |
| Number of grid points $N_x, (N_y^f + N_y^p), N_z$ | 149, (129+16), 129 | 149, (129+20), 129 | 149, (129+20), 129 | 129, 129, 129 |



DNS of turbulent channel flow

Governing equations

Continuity equation

$$\nabla \cdot \mathbf{u} = 0$$

Momentum equation

$$\frac{D\mathbf{u}}{Dt} = -\nabla p' + \nu \nabla^2 \mathbf{u} + (1 - \varphi) \mathbf{S}$$

Numerical scheme

➤ Spatial discretization scheme

Finite Volume Method

➤ Time advancement

Implicit Euler method (1st)

➤ Poisson equation

PISO algorithm



OpenFOAM®

Porous model

Darcy-Forchheimer equation

$$\mathbf{S} = -\frac{\nu}{K} \mathbf{u}_m - 2 \frac{c_f}{\sqrt{K}} |\mathbf{u}_m| \mathbf{u}_m$$

φ : Porosity 0.80

K : Permeability 0.02 [mm²]

c_f : Forcheheimer coefficient 0.17

Drag reduction ratio

$$DR[\%] = \left(1 - \frac{C_f^p}{C_f^0} \right) \times 100$$

C_f^p : Friction coefficient over porous wall
 C_f^0 : Friction coefficient over flat wall

FIK identity^[1]

$$C_f = \underbrace{\frac{12}{Re_b}}_{\text{Viscous term}} + \underbrace{12 \int_0^1 2(1-y)(\overline{-u'v'}) dy}_{\text{Turbulent term}}$$

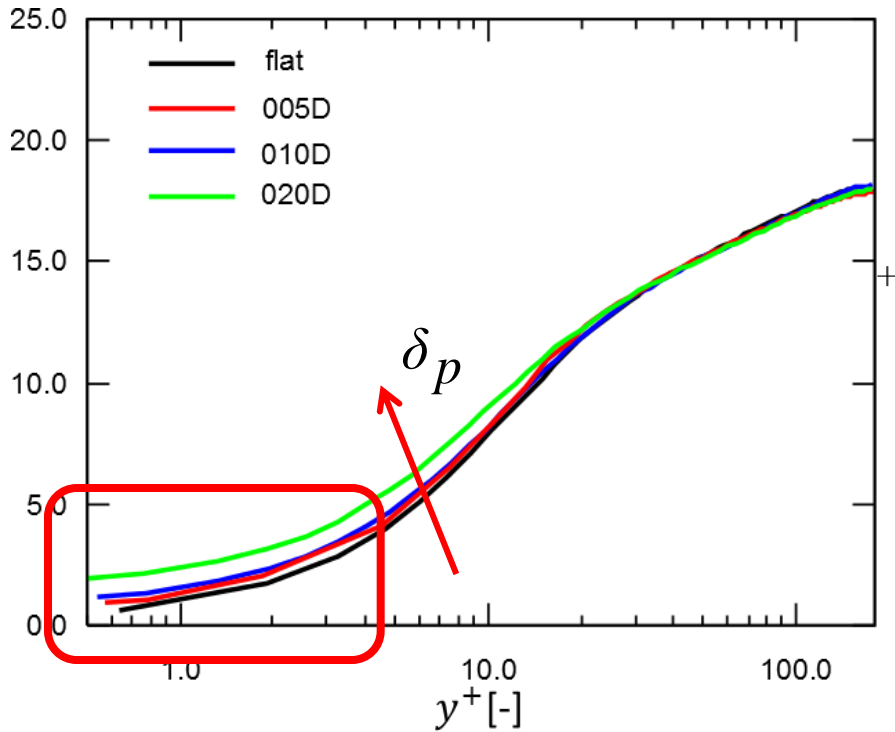
Viscous term and Turbulent term

| Case | $C_f \times 10^3$ | DR [%] | δ_p^+ |
|------|-------------------|--------|--------------|
| 5%D | 6.55 | +9.6 | 9 |
| 10%D | 7.16 | +1.3 | 18 |
| 20%D | 7.56 | -4.3 | 37 |
| Flat | 7.25 | | |

[1] Fukagata, K., Iwamoto, K. and Kasagi, N., Phys. Fluids, 14 (2002), pp.73-76

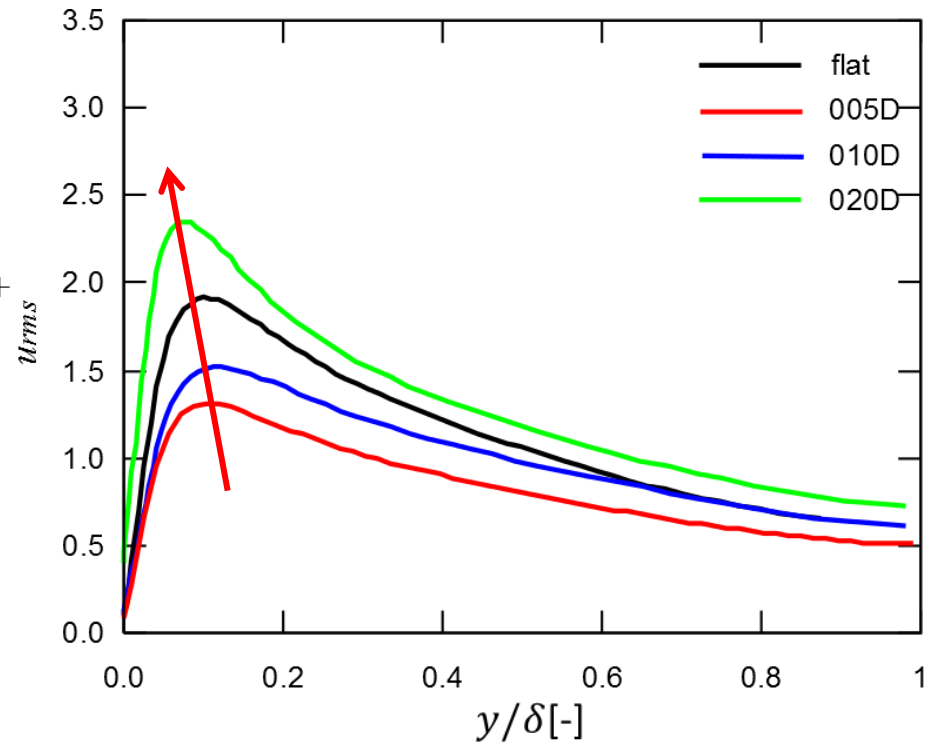
Turbulent statistics

Mean velocity profiles



Slip velocity occurred over porous walls.

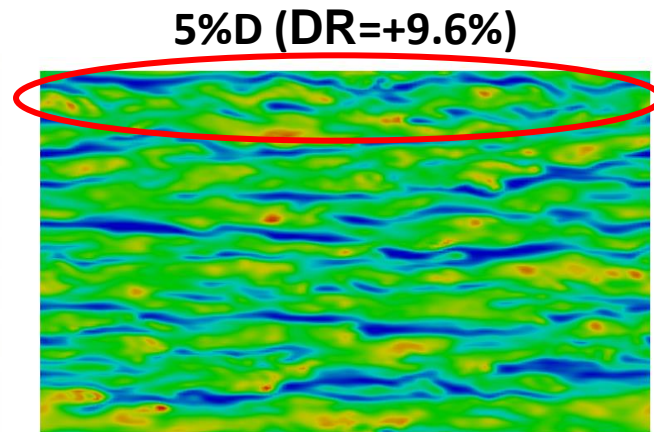
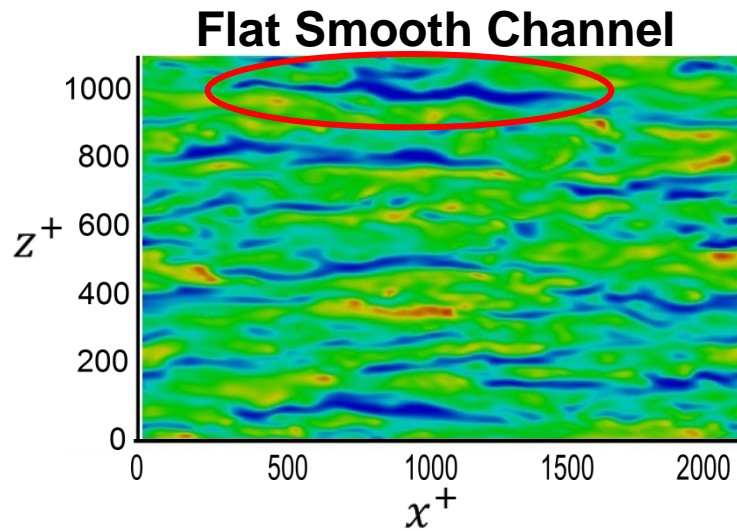
Turbulence intensity



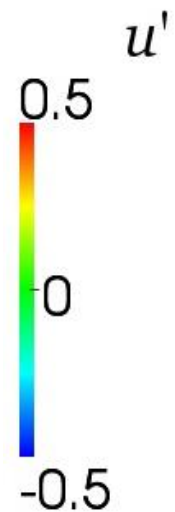
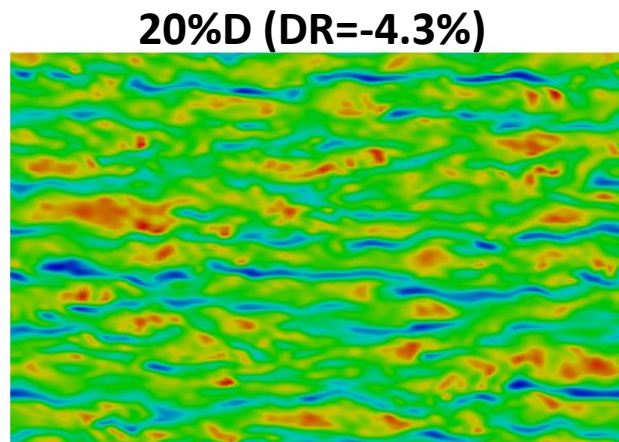
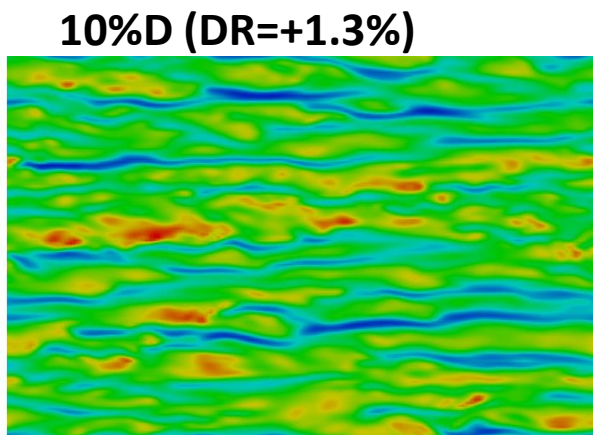
Turbulence intensity became stronger.

Turbulent structure – Streak structure

Snapshot of velocity fluctuation at $y^+ \sim 20$



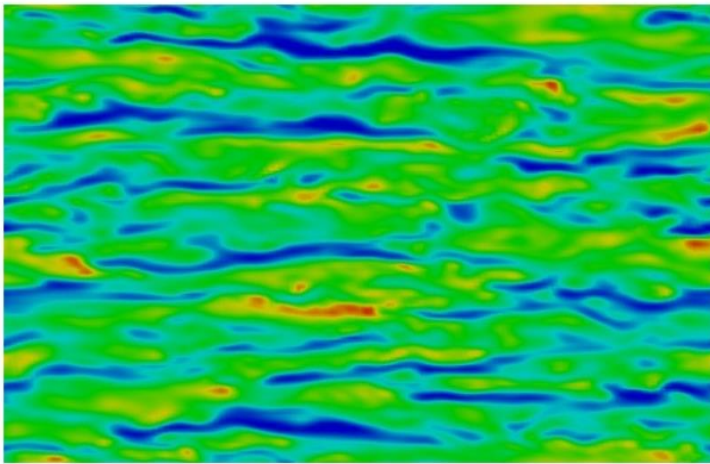
Longer streaky structure



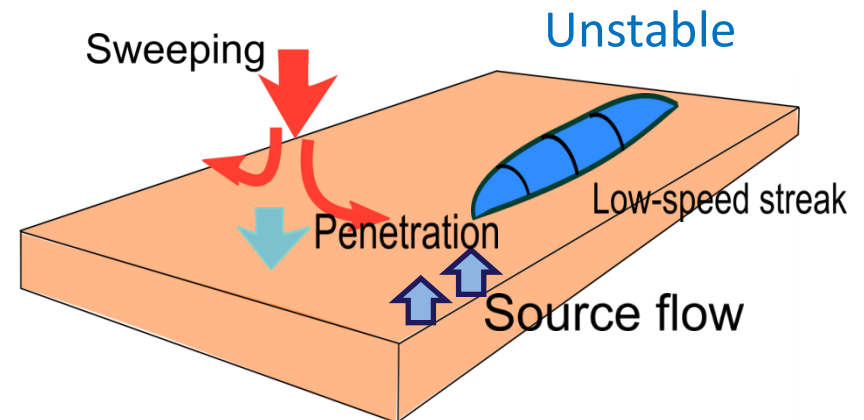
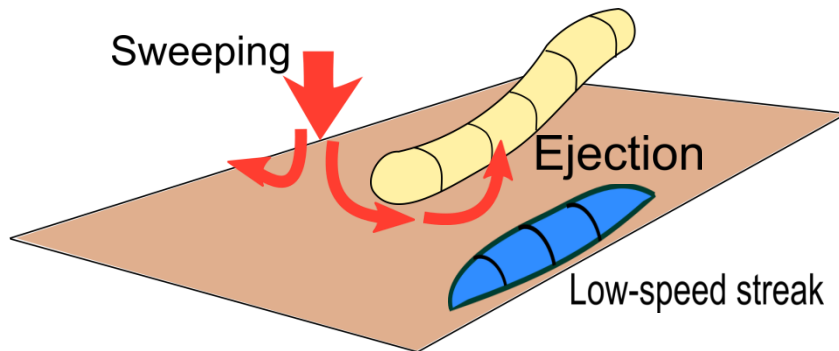
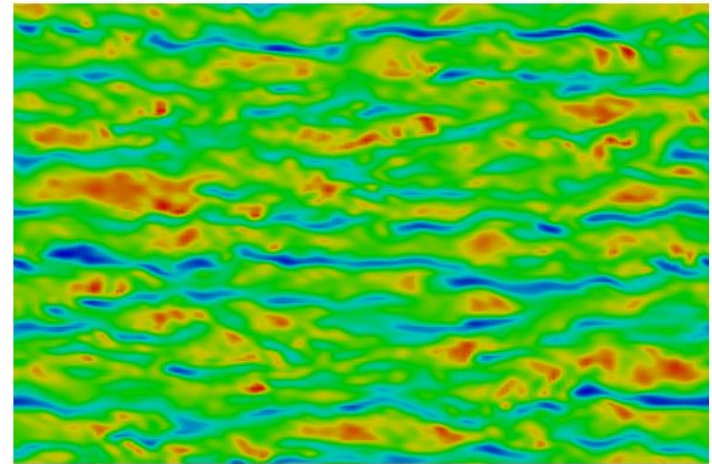
Effect of wall thickness

The mechanism of vortex generation

Flat wall



Porous wall

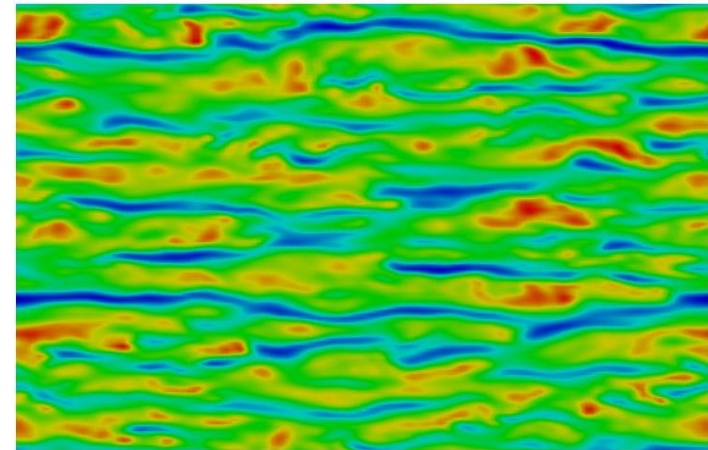
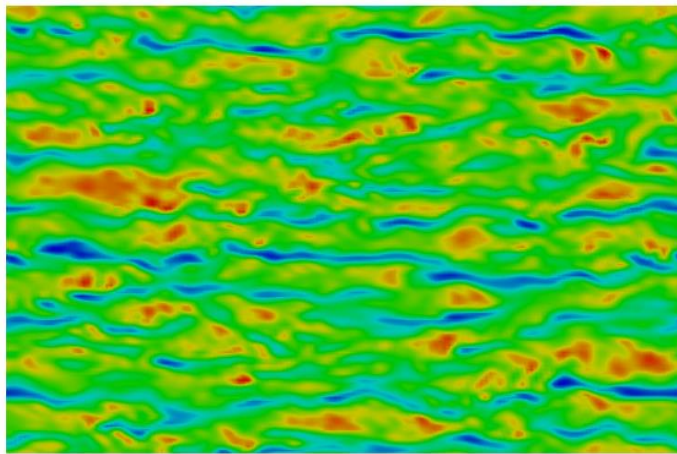


Effect of wall thickness

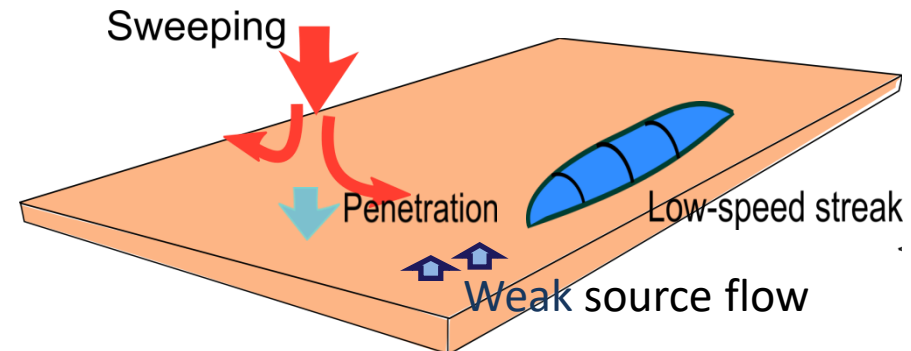
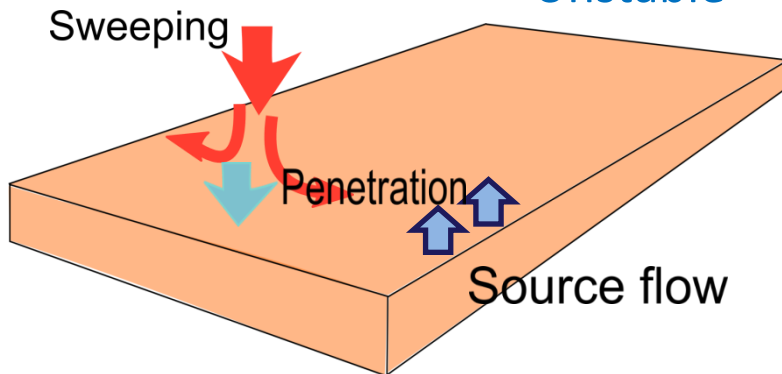
The mechanism of vortex generation and decaying

Thick Porous wall (Drag increasing)

Thin porous wall (Drag reducing)



Unstable

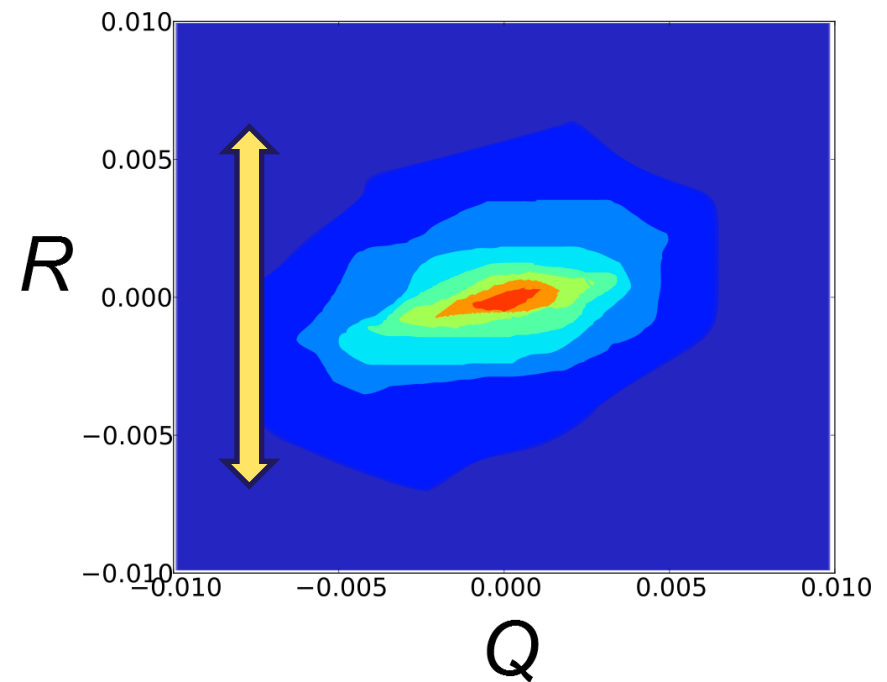
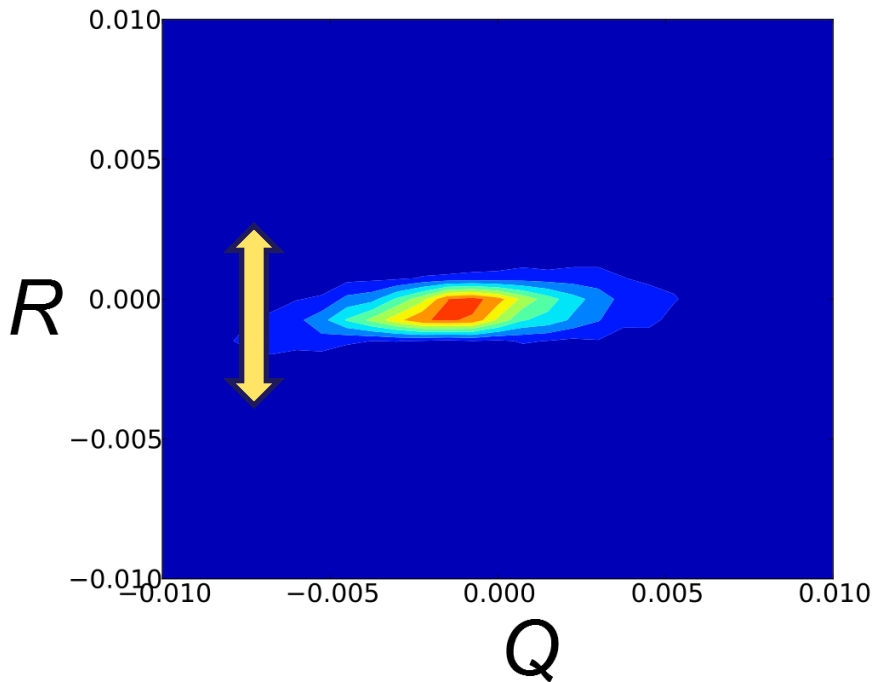


Joint Probability Density Function (JPDF)

The mechanism of vortex generation and decaying

Thin porous wall 5%D (Drag reducing)

Thick Porous wall 20%D (Drag increasing)



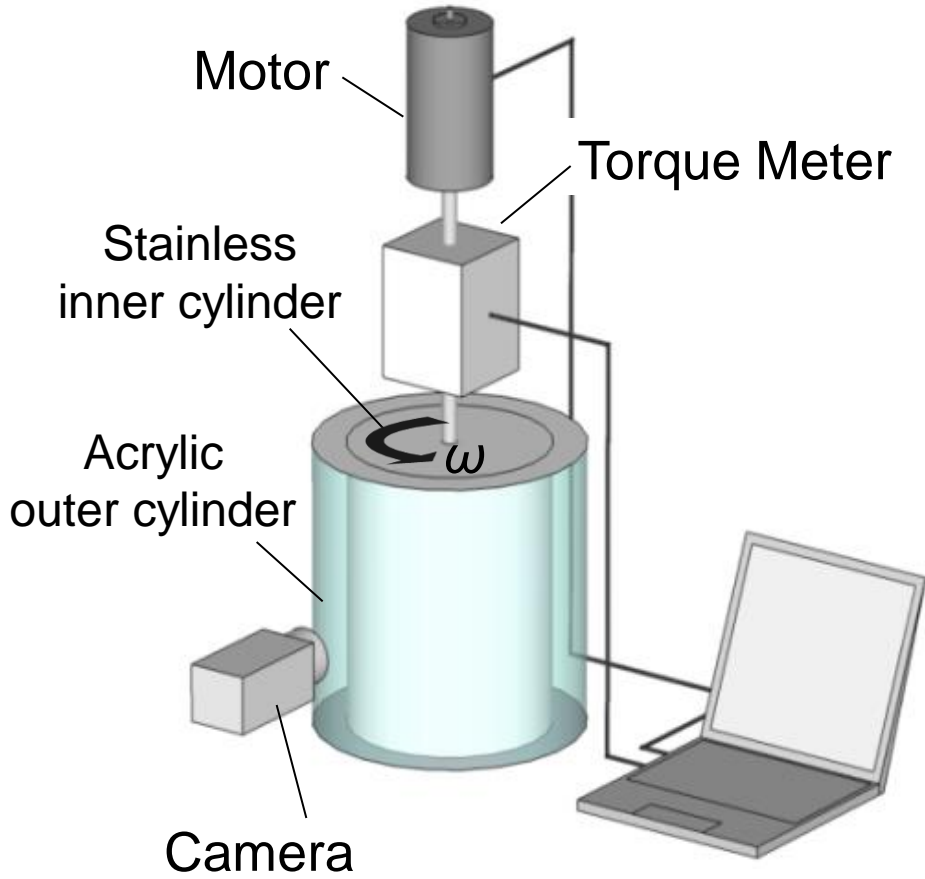
Summary of topic 4

- The direct numerical simulation on a channel with porous walls which had varying wall thickness were carried out.
- The drag reduction was achieved over the **thinnest porous wall**, and in that case, turbulent intensity became weaker.
- The turbulent structures suggested that the relationship between the **intensity** of sweep (or ejection) and the **thickness of porous wall** was an important factor for drag reduction.

5. Experimental evaluation of drag reduction: Taylor-Couette flow

Experimental setup

Rotating cylinder facility



r_i : radius of inner cylinder [m]
 r_o : radius of outer cylinder [m]
 L : height [m]
 ω : angular velocity [m]
 d : gap between the cylinders [m]
 ν : kinetic viscosity [m^2/s]
 ρ : density [kg/m^3]
 T : torque of inner cylinder [Nm]

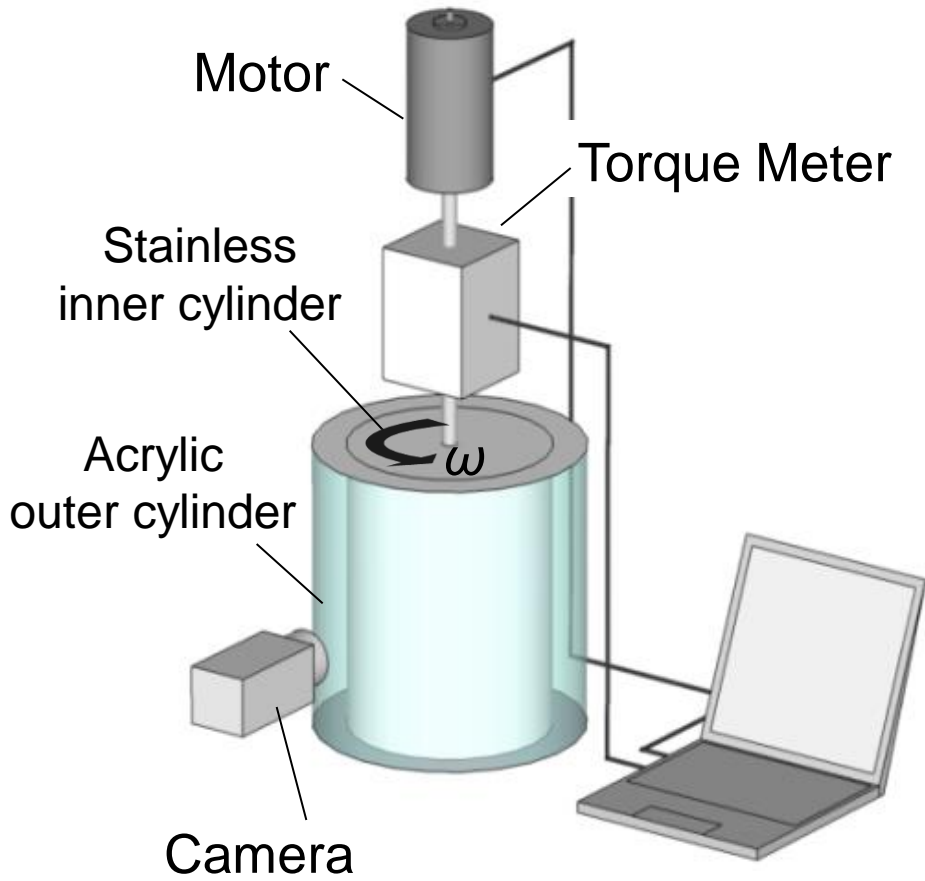
$r_i = 48 \text{ mm}$
 $r_o = 64 \text{ mm}$
 $L = 128 \text{ mm}$

Reynolds number: $Re = \frac{r_i \omega d}{\nu}$

Nondimensionalized torque: $G \equiv \frac{T}{\rho \nu^2 L}$

Flow pattern

Rotating cylinder facility



Reynolds number: $Re = \frac{r_i \omega d}{\nu}$

$Re = 4.2 \times 10^3$



Steady vortexes

$Re = 8.8 \times 10^3$

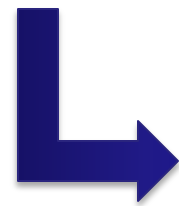


Wavy vortexes

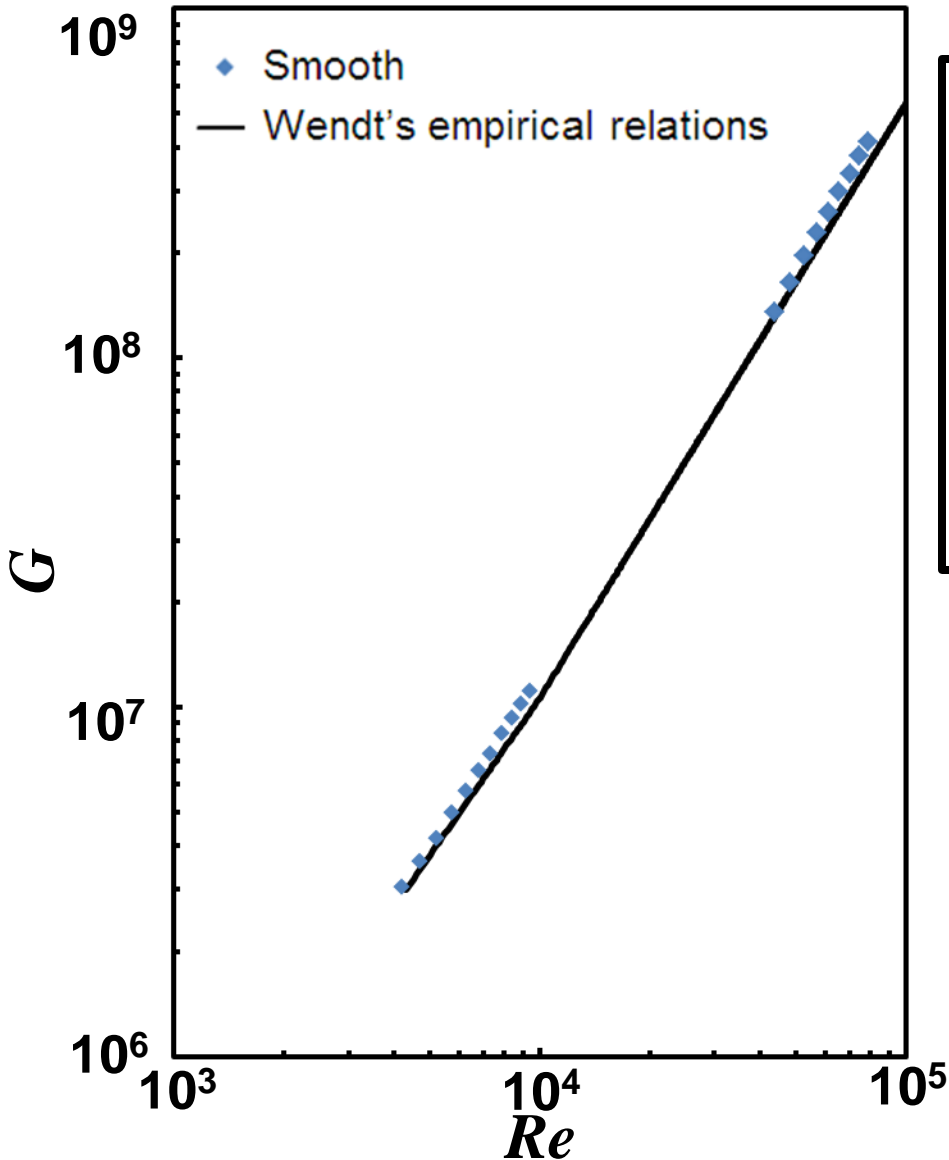
$Re = 4.4 \times 10^4$



Disturbed flow



Validity of measurement



Wendt's empirical relations

$$G = \begin{cases} 1.45 \frac{\eta^{3/2}}{(1-\eta)^{7/4}} Re^{1.5} & \text{for } 4 \times 10^2 < Re < 10^4 \\ 0.23 \frac{\eta^{3/2}}{(1-\eta)^{7/4}} Re^{1.7} & \text{for } 10^4 < Re < 10^5 \end{cases}$$

η : radius ratio r_i / r_o

F. Wendt, Ingenieur-Archiv. **4**, 577 (1933).

Experimental conditions

Test cylinders



Smooth



Cured



Hydrogel

Thickness of primer

Total : $220 \mu m$

1st layer : $140 \mu m$

2nd layer : $80 \mu m$

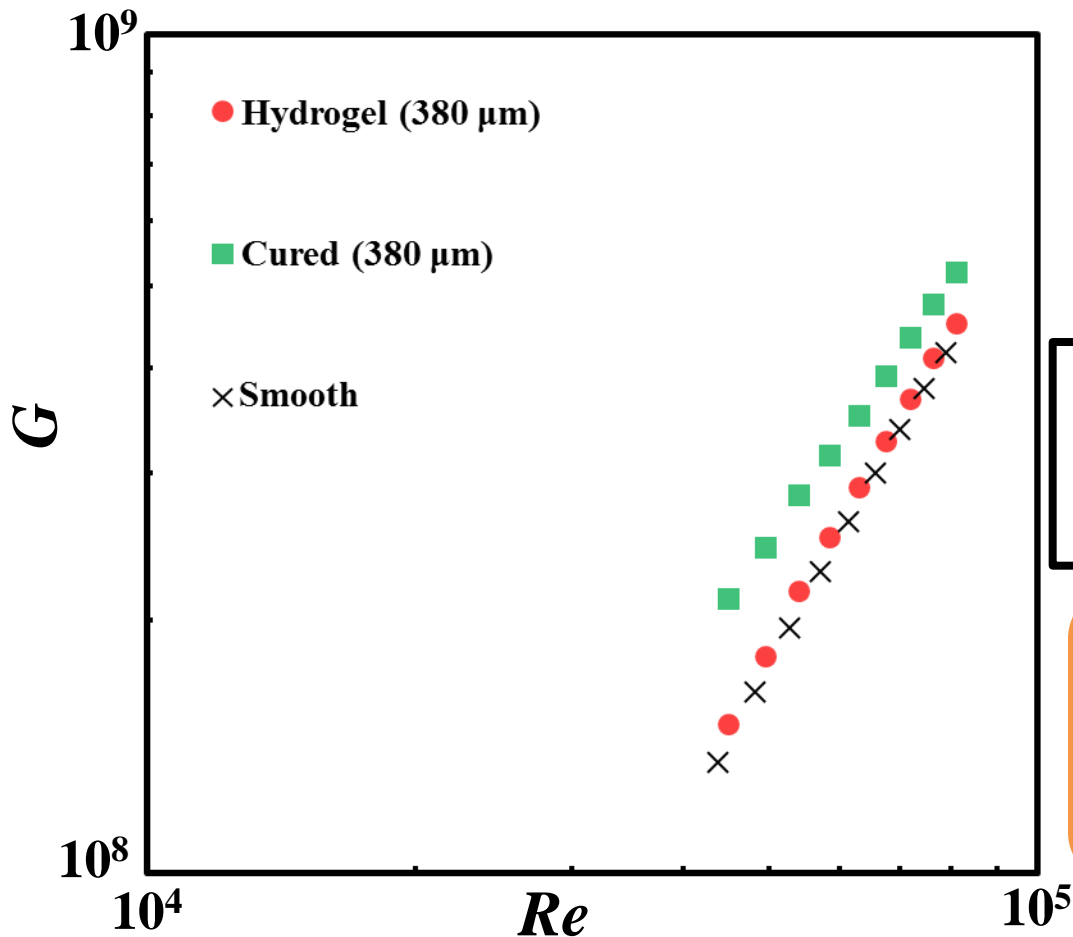
Thickness of coating

| | Thick | Thin |
|----------|-------------|-------------|
| Cured | $380 \mu m$ | $240 \mu m$ |
| Hydrogel | $380 \mu m$ | $240 \mu m$ |

Range of Re

$$4.4 \times 10^4 < Re < 8.1 \times 10^4$$

Drag reduction effect



Reynolds number

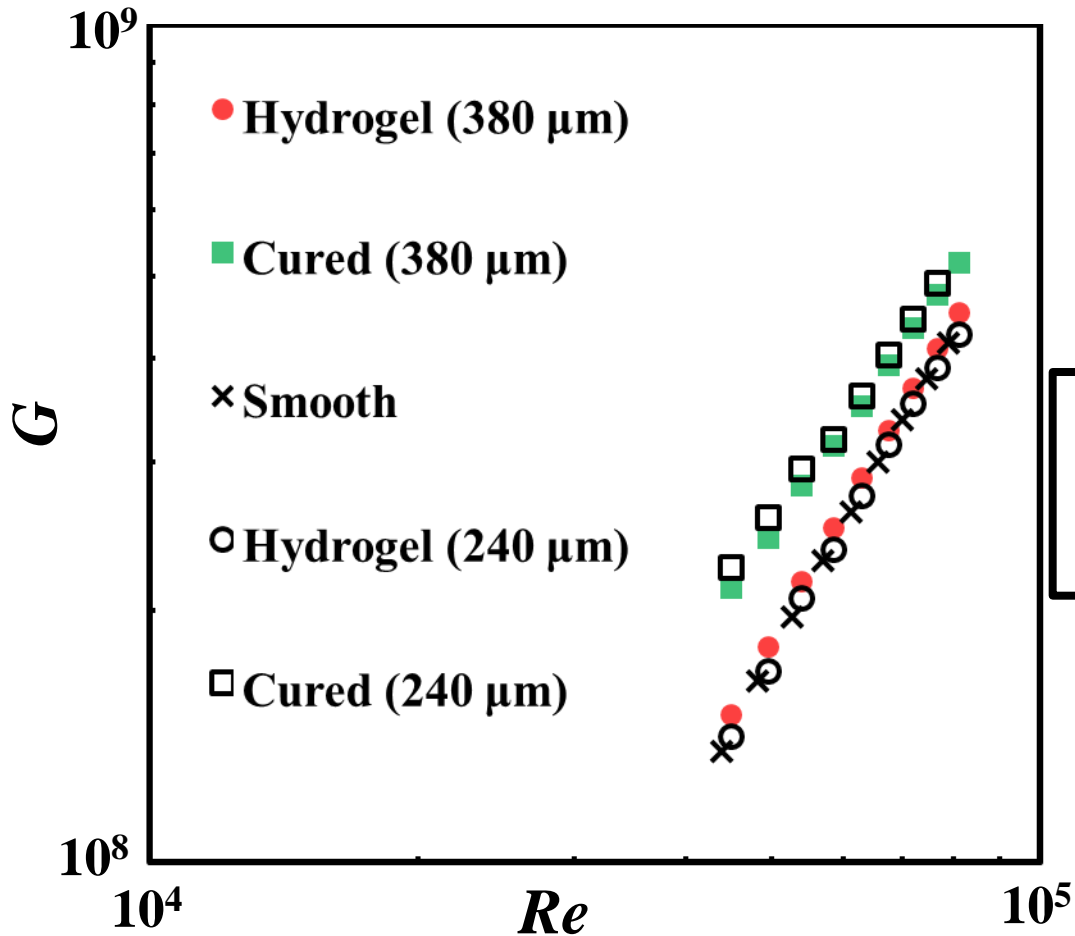
$$Re = \frac{r_i \omega d}{\nu}$$

Nondimensionalized torque

$$G \equiv \frac{T}{\rho v^2 L}$$

Torque G of hydrogel coating was smaller than that of Cured coating.

Drag reduction effect



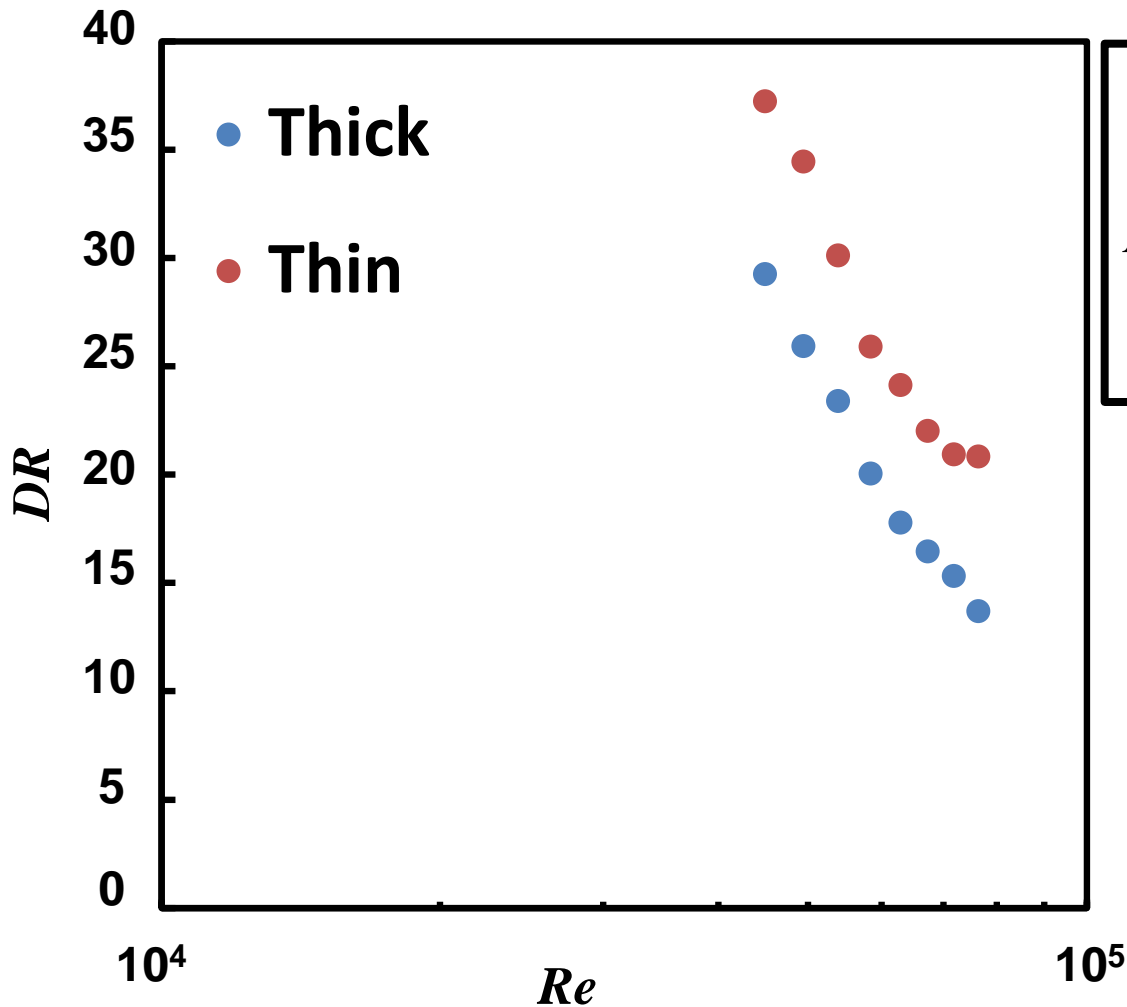
Reynolds number

$$Re = \frac{r_i \omega d}{\nu}$$

Nondimensionalized torque

$$G \equiv \frac{T}{\rho v^2 L}$$

Relation with DR and Re



Drag Reduction Ratio

$$DR = \frac{G_{Cured} - G_{Hydrogel}}{G_{Cured}} \times 100$$

$$\Delta DR \sim 7\%$$

Drag reduction effect of thin hydrogel was larger than thick one.